U.S. Department
of Transportation
**Federal Railroad
Administration**

Analysis of Lateral Rail Restraint

Office of Research and
Development
Washington DC 20590

David Jeong
Michael Coltman

Transportation Systems Center
Cambridge MA 02142

FRA/ORD-83/15
DOT-TSC-FRA-83-4

September 1983
Final Report

NOTICE

This document is disseminated under the sponsorship of the Department of Transportation in the interest of information exchange. The United States Government assumes no liability for its contents or use thereof.

NOTICE

The United States Government does not endorse products or manufacturers. Trade or manufacturers' names appear herein solely because they are considered essential to the object of this report.

Technical Report Documentation Page

1. Report No.	2. Government Accession No.	3. Recipient's Catalog No.
FRA/ORD-83/15		

4. Title and Subtitle	5. Report Date
ANALYSIS OF LATERAL RAIL RESTRAINT	September 1983
	6. Performing Organization Code TSC/DTS-76
7. Author(s) David Jeong and Michael Coltman	8. Performing Organization Report No. DOT-TSC-FRA-83-4
9. Performing Organization Name and Address U.S. Department of Transportation Research and Special Programs Administration Transportation Systems Center Cambridge MA 02142	10. Work Unit No. (TRAIS) RR319/R3304 11. Contract or Grant No.
12. Sponsoring Agency Name and Address U.S. Department of Transportation Federal Railroad Administration Office of Research and Development Washington DC 20590	13. Type of Report and Period Covered Final Report June 1980-September 1980 14. Sponsoring Agency Code RRD-10

15. Supplementary Notes

16. Abstract

Rail restraint failure is one of the most prevalent derailment modes in railroad operation. Analytical and experimental investigations of track gauge widening have been undertaken by the Transportation Systems Center in support of the Federal Railroad Administration's Track Safety Research Program to establish performance based track safety specifications.

This report deals with the analysis of lateral rail strength using the results of experimental investigations and a nonlinear rail response model. Part of the analysis involves the parametric study of the influence of track parameters on lateral rail restraint. These parameters include rail size, rail support characteristics, and wheel versus truck loading. Based on these results, safety limits on allowable rail restraint degradation for low speed track are presented.

17. Key Words	18. Distribution Statement
RAIL RESTRAINT, GAUGE WIDENING, RAIL DEFLECTION	DOCUMENT IS AVAILABLE TO THE PUBLIC THROUGH THE NATIONAL TECHNICAL INFORMATION SERVICE, SPRINGFIELD, VIRGINIA 22161

19. Security Classif. (of this report)	20. Security Classif. (of this page)	21. No. of Pages	22. Price
Unclassified	Unclassified	88	

Form DOT F 1700.7 (8-72) Reproduction of completed page authorized

PREFACE

In support of the Federal Railroad Administration's (FRA) Track Safety Research Program, the Transportation Systems Center is conducting research to develop the engineering basis for more effective track safety guidelines and specifications. The intent of these specifications is to ensure safe train operations while allowing the industry increased flexibilty for cost effective track engineering and maintenance practices.

One of the major safety issues currently under investigation under this program deals with lateral rail restraint. The work reported here is part of this investigation dealing with the analysis of experimental data using a nonlinear rail response model. The analysis entails identification of support conditions for the model characterizing the track on which the testing was performed. Once these support conditions are identified the influence of several track parameters is extrapolated. These parameters include rail size, missing support and wheel versus truck loading.

METRIC CONVERSION FACTORS

Approximate Conversions to Metric Measures

Symbol	When You Know	Multiply by	To Find	Symbol
		LENGTH		
in	inches	*2.5	centimeters	cm
ft	feet	30	centimeters	cm
yd	yards	0.9	meters	m
mi	miles	1.6	kilometers	km
		AREA		
in^2	square inches	6.5	square centimeters	cm^2
ft^2	square feet	0.09	square meters	m^2
yd^2	square yards	0.8	square meters	m^2
mi^2	square miles	2.6	square kilometers	km^2
	acres	0.4	hectares	ha
		MASS (weight)		
oz	ounces	28	grams	g
lb	pounds	0.45	kilograms	kg
	short tons (2000 lb)	0.9	tonnes	t
		VOLUME		
tsp	teaspoons	5	milliliters	ml
Tbsp	tablespoons	15	milliliters	ml
fl oz	fluid ounces	30	milliliters	ml
c	cups	0.24	liters	l
pt	pints	0.47	liters	l
qt	quarts	0.96	liters	l
gal	gallons	3.8	liters	l
ft^3	cubic feet	0.03	cubic meters	m^3
yd^3	cubic yards	0.76	cubic meters	m^3
		TEMPERATURE (exact)		
°F	Fahrenheit temperature	5/9 (after subtracting 32)	Celsius temperature	°C

*1 in. = 2.54 cm (exactly). For other exact conversions and more detail tables see NBS Misc. Publ. 286, Units of Weight and Measures. Price $2.25 SD Catalog

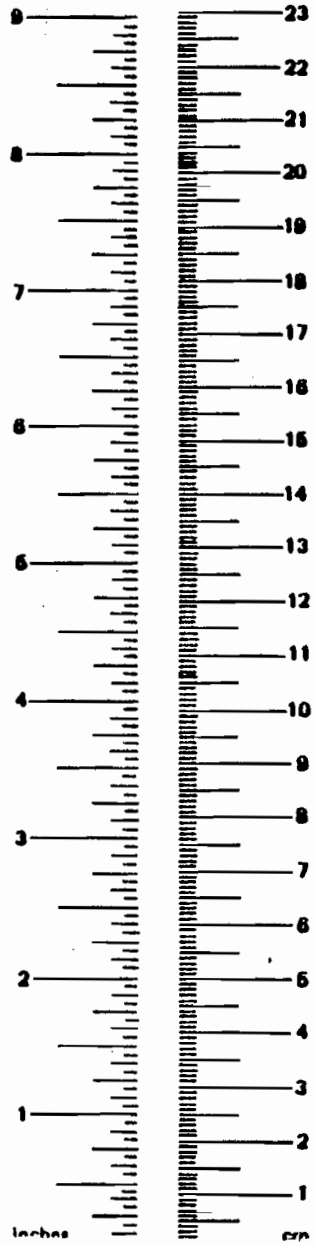

Approximate Conversions from Metric Measures

Symbol	When You Know	Multiply by	To Find	Symbol
		LENGTH		
mm	millimeters	0.04	inches	in
cm	centimeters	0.4	inches	in
m	meters	3.3	feet	ft
m	meters	1.1	yards	yd
km	kilometers	0.6	miles	mi
		AREA		
cm^2	square centimeters	0.16	square inches	in^2
m^2	square meters	1.2	square yards	yd^2
km^2	square kilometers	0.4	square miles	mi^2
ha	hectares (10,000 m^2)	2.5	acres	
		MASS (weight)		
g	grams	0.036	ounces	oz
kg	kilograms	2.2	pounds	lb
t	tonnes (1000 kg)	1.1	short tons	
		VOLUME		
ml	milliliters	0.03	fluid ounces	fl oz
l	liters	2.1	pints	pt
l	liters	1.06	quarts	qt
l	liters	0.26	gallons	gal
m^3	cubic meters	36	cubic feet	ft^3
m^3	cubic meters	1.3	cubic yards	yd^3
		TEMPERATURE (exact)		
°C	Celsius temperature	9/5 (then add 32)	Fahrenheit temperature	°F

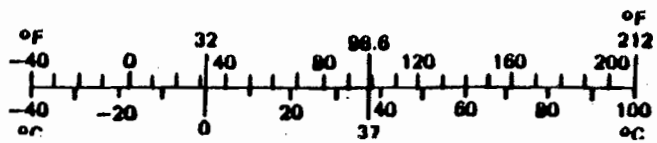

TABLE OF CONTENTS

LIST OF FIGURES

LIST OF FIGURES (continued)

LIST OF TABLES

SUMMARY

Rail restraint failure is the cause of a large number of derailments on U.S. track. In the past considerable attention has been given to investigating the factors contributing to rail rotation. However, recent studies [4] have turned the focus of attention from rail rollover to the lateral translation of track that is structurally weak in response to the application of substantial lateral load.

Research has been conducted under the Federal Railroad Administration's Track Safety Research Program to establish performance based track safety specifications in the area of lateral rail restraint. Under this program the Transportation Systems Center has supported the FRA by performing a set of tasks intended to enhance the understanding of the gauge widening phenomena, in view of recent studies. These tasks have involved: (a) the performance of rail restraint tests on track typical of low speed operation (i.e., speeds in the range of 5-25 mph), and (b) the development of a nonlinear rail response model that is convenient to relate stiffness components to the experimental results. These tasks were performed during the summer of 1980 (June to September).

This report deals with the analysis of lateral rail restraint using the data obtained through the gauge widening testing and the rail response model. The rail response model is used to identify the support characteristics representative of track in the low speed regime. Once the support characteristics have been identified a parametric study of the influence of several track parameters can be conducted to extrapolate the results. These parameters include rail size, missing support, and wheel versus truck loading. The results of the analysis are used to define lower bound behavior and "minimally acceptable" rail strength limits. A report by Kish, Dzwonczyk, and Jeong [17] specifically describes the experimental part of this investigation.

Key parameters influencing the strength and failure mechanism of gauge widening are presented. Also, based on the obtained analytical and experimental results, a prototype performance based safety specification for the allowable rail restraint degradation of low speed track is presented. It is pointed out that the same procedure can be used to extrapolate results for higher speed track.

1. INTRODUCTION - BACKGROUND

The loss of adequate rail restraint, resulting in gauge widening, is a major track failure mode and the cause of a large number of derailments on U.S. track. Accident statistics indicate that approximately 20-25% of all track induced accidents are attributable to rail restraint failure. Furthermore, these accidents predominantly occur on track limited to a 5-25 mph regime of operation and with substantial geometric and structural imperfections and missing or poorly functioning ties. The reduction of the number of these accidents through maintenance and better performance based specifications has been a strong concern to the railroad community.

The problem of gauge widening and rail overturning has been investigated both analytically and experimentally.

Experimental determination of lateral strength of track has been attempted by several means in the last 10 years [1,2,3]. The characteristics of these investigations are summarized in Table 1.1. All of these studies observed that the lateral strength is dependent on the level of vertical load. Other major findings of these tests can be summarized as follows:

1. Lines of constant gauge widening in the lateral versus vertical load curve appear to be straight parallel lines. Damage to the track is exhibited by a shift in these lines.

2. A lateral load versus railhead lateral deflection curve under constant vertical load typically exhibits 4 regimes of deformation. Each regime has a specific response associated with it.

3. Typically, three different gauge widening failure modes have been observed:

   MODE A: failure due to rail rotation (rail rollover)

   MODE B: failure due to rail translation (rail shift)

   MODE C: combination of modes A and B. It appears that mode C occurs under greater vertical loads and that mode A occurs under smaller vertical loads.

4. Total deformation of the rail is a combination of elastic deformation, rigid body translation and rotation.

TABLE 1.1 - RAIL RESTRAINT CAPACITY AVAILABLE MEASURED DATA

SOURCE	TRACK CONDITION	TEST CONDITIONS	TEST/DATA LIMITATIONS
ON FIELD TEST 1972 (LUNDGREN & SCOTT)	o TANGENT YARD TRACK o GOOD (NEW) TIES o RAIL SIZE: 80, 85, 100, 115 AND 130#	o LOADED CAR INDUCED VERTICAL LOADS (9.4, 17.7, 26.7, 32.6 KIPS) o SPECIAL LATERAL LOADING HEAD	o DID NOT REPRESENT WEAK OR MINIMUM TRACK CONDITION o NON-REALISTIC LOAD APPLICATION RESULTING IN EXCESSIVE OVERTURNING MOMENT.
AAR TRACK LAB TESTS (ZAREMBSKI & CIORCS)	o 136# RE RAIL o "NEW" TIES: "DEGRADED" BY SPIKE PULL-OUT	o CONSTRAINED TWO POINT CONTACT o "DAMAGED" TRACK BY CYCLING LOADS AND DEFLECTIONS o "WEAKENED" TRACK AND SPECIAL TESTS (MULTIPLE AND AXIAL LOADS)	o EXCESSIVE OVERTURNING MOMENT DUE TO CONSTANT TWO POINT CONTACT o NEW TIES "DEGRADED" BY SPIKE PULL OUT MAY NOT BE TYPICAL OF MINIMAL TRACK
TTD "DECAROTOR" TESTS ON SR (AAR/TSC/SR)	o 90# RAIL IN YARD o 132# RAIL IN MAIN-LINE TRACK WITH NEW TIES AND 5 YEAR TIES	o UTILIZES 12" LOAD WHEEL o STATIONARY AND MOVING o VERTICAL LOAD TO 15 KIPS o LATERAL LOAD TO 10 KIPS	o LOADS AND DEFLECTIONS TOO LIMITED FOR RAIL RESTRAINT ANALYSIS o TO DATE, MINIMUM STATIONARY DATA AVAILABLE

However, since each of these sets of tests was conducted with some specific features of interest, such as load level or artificially degraded track, none of them is representative of or can readily be interpreted as characteristic of weak or poor track.

Furthermore, the mechanics of gauge widening have not been well understood. Analytical studies of the problem have been largely exploratory in nature. Such influences as the effect of axial load, nonlinear support and dynamic loads have been examined in an attempt to account for what has been viewed as unexpectedly weak track.

A survey of the work performed in the area of rail overturning, both experimental and analytical has been written by Zarembski [5]. It was pointed out in this survey that the first attempt to analytically define the problem of rail roll was made by Timoshenko in 1926 [6].

More recently, Bhatti [7] utilized dynamic equilibrium to determine lateral deflections and rotations of rail subjected to time dependent lateral and vertical forces and constant axial force. Equations of motion were developed and solved using Galerkin's Method and Mode Superposition. Chu and Wang [8] considered effects of nonlinear spring resistance through a finite element model. Load eccentricity was taken into account as well as axial, vertical, and lateral forces. A previous analysis by Chu and Wang [9] utilized a finite difference approach to solve Timoshenko's equations which were modified to include constant axial loading and nonlinear effects of interacting moments.

Research conducted by the Transportation Systems Center for the Federal Railroad Administration has involved the development of data and technical information required for the specification of safety performance standards for rail restraint. In view of the previous analytical and experimental work performed in the areas of gauge widening a set of tasks have been undertaken and described in this document. These tasks are described by the following:

1. The determination of realistic component response parameters through an appropriate test procedure. These component parameters include spike pullout and bending resistances and tie plate sliding resistance.

2. The development of an analytical model to predict the widening of the track gauge and rail restraint degradation.

3. Tests for rail restraint strength determination to supplement 1. and 2.

Once the relationships between the component parameters and gauge widening resistances, and that between deterioration of components and rail constraint are obtained, it will be possible to replace costly and time consuming gauge widening tests by cheaper and quicker component performance tests under various combinations of loads and environments. With these relationships, an assessment of the rail restraint strength and deterioration can be made.

The purpose of this report is to describe the parametric studies and analyses performed in determining these relationships using the analytical model and the test data. Results of these studies are presented as well as conclusions, applications of the study to introduce a performance based safety specification, and recommendations for future work in this research area.

2. DESCRIPTION OF THE MODEL

2.1 General

In this study a finite element model was formulated to analytically investigate the problem of gauge widening. This model represents the rail as a beam supported at tie spacing intervals by preceived linear vertical and lateral springs which are attached to the base of the rail (see Figure 2.1). These springs are intended to be equivalent to the support of the rail provided by the tie-fastener combination. Displacements of the rail relative to the tie, due to vertical and lateral loads applied at the crown of the rail, are predicted by the model.

The finite element method typically solves the equation:

$$\{F\} = [K]\{\delta\}$$

where $\{F\}$ = applied force vector
$[K]$ = global stiffness matrix
$\{\delta\}$ = nodal displacement vector.

The global stiffness matrix, [K], is computed on the basis of linear elastic assumptions. In the finite element model developed in this study the global stiffness matrix is computed to include the effects of the piecewise linear springs. The stiffness matrix, [K] then becomes a function of the nodal displacements. The applied force vector {F} is also a function of the displacements due to geometric considerations. Therefore, the model is nonlinear and an iterative method is used in the solution. These nonlinearities and other considerations are discussed in the following section.

2.2 Finite Element Considerations

2.2.1 Beam Element

The rail is modeled as a series of segments or beam elements consisting of a pair of nodes each, i.e., there are 2 nodes per element. At each of these nodes a set of local coordinates is established. These local coordinates consist of three axes (representing three dimensions), with 2 degrees of freedom per axis. Therefore, there are 6 degrees of freedom per node. The

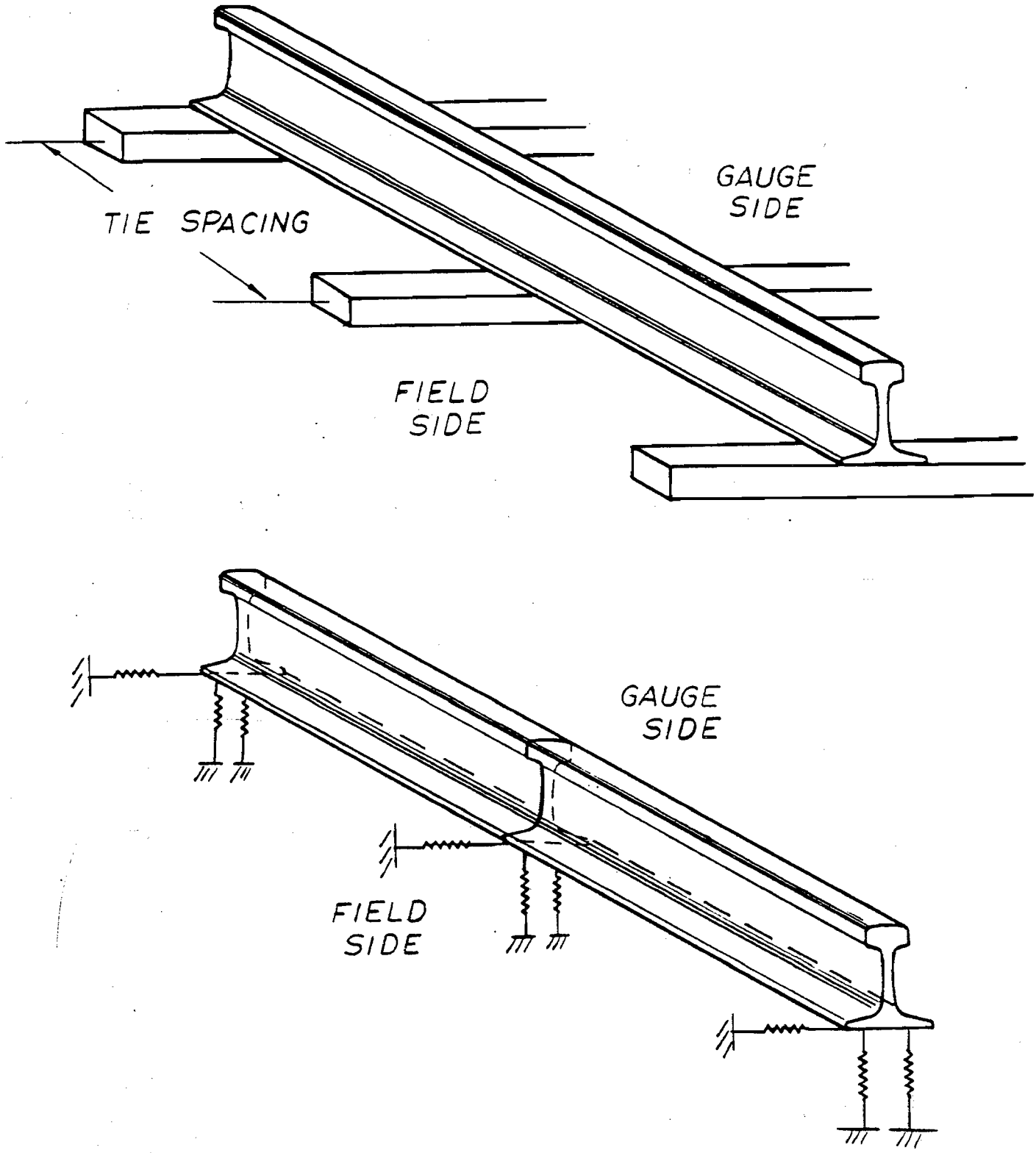

FIG. 2.1 - SCHEMATIC OF ANALYTICAL MODEL

local coordinates are used along with the beam element strain energy to derive an element stiffness matrix for that beam element. Finally, the local coordinates are then used to relate the individual beam element stiffnesses to a global local coordinate system and a global stiffness matrix. The global or master stiffness matrix represents the beam stiffness properties of a rail as modeled as a beam.

Each rail segment is treated as a linear elastic beam element subjected to a combination of vertical, lateral, and torsional loads applied at the shear center of the rail cross-section (see Figure 2.2). Since the rail has an unsymmetric cross-section, both St. Venant torsion and warping must be considered when twisting loads are applied to the rail. In addition, lateral bending and twisting are coupled when the tie-fastener support shown schematically in Figure 2.3b operates at the rail base. This coupling has been discussed by Timoshenko and Langer [10] for continuously supported rail and the extension to coupling with vertical bending for discretely supported rail subject to flanging loads by McConnell and Perlman [11].

The stiffness of a rail element can then be characterized by

- vertical and lateral area moments of inertia
- Young's modulus and shear modulus
- torsional rigidity and warping constants
- geometric dimensions of the rail cross section (such as location of the applied loads, shear center, rail height, rail base width, etc.)

Numerical values of the necessary area and dimensional parameters have been tabulated for a range of common rail weights in Reference 12.

A set of x-y-z axes are shown in Figure 2.4a for a beam element. Each axis has an associated pair of displacement components. The x axis represents the axial or longitudinal direction; y represents lateral; and z represents vertical. Therefore, the displacement vector for the beam element shown in Figure 2.5 can be written:

$$\{\delta_e\} = [w_i \; v_i \; \phi_i \; \theta_i \; \psi_i \; x_i \; w_j \; v_j \; \phi_j \; \theta_j \; \psi_j \; x_j]^T$$

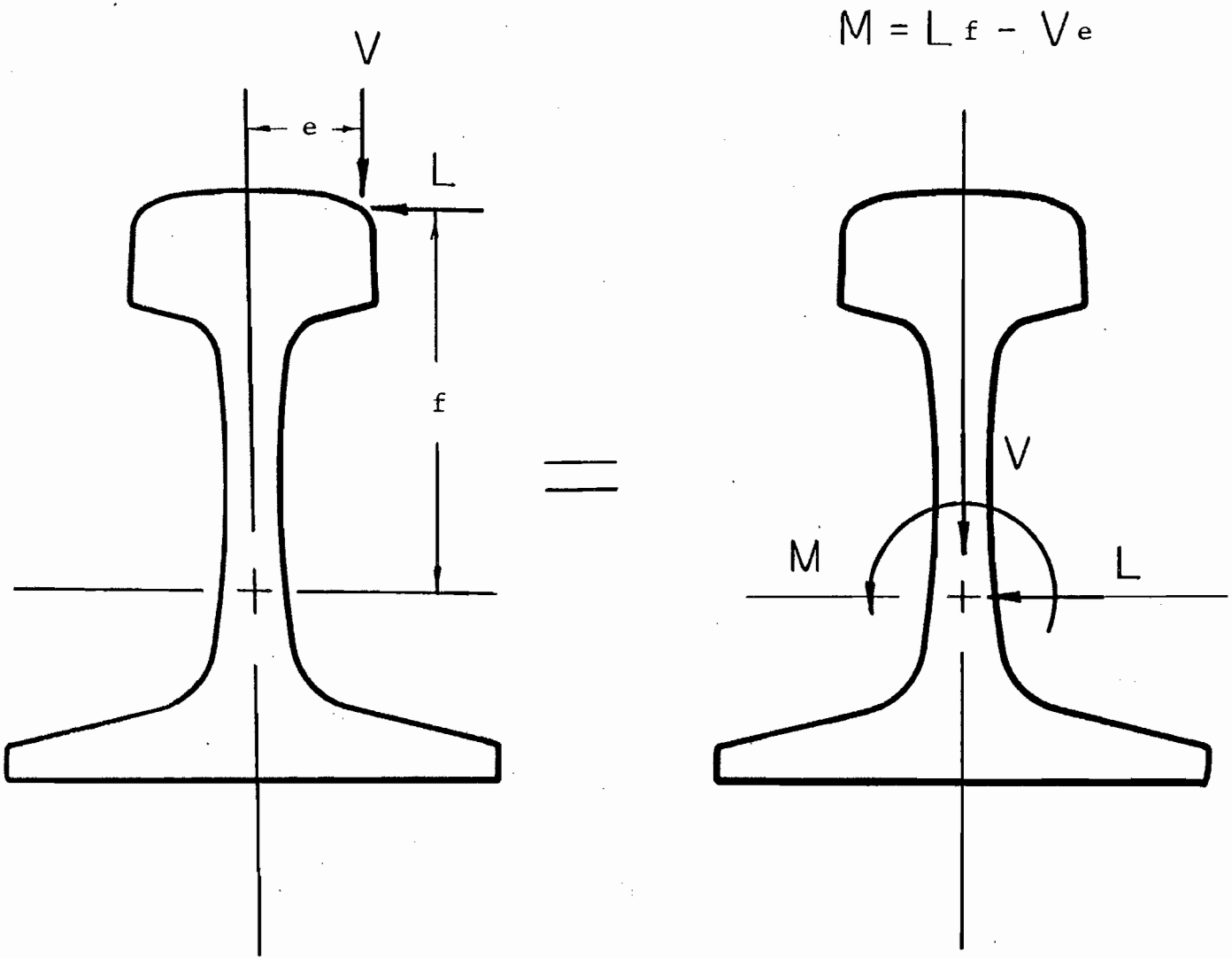

FIG. 2.2 - EQUIVALENT STATIC LOADING

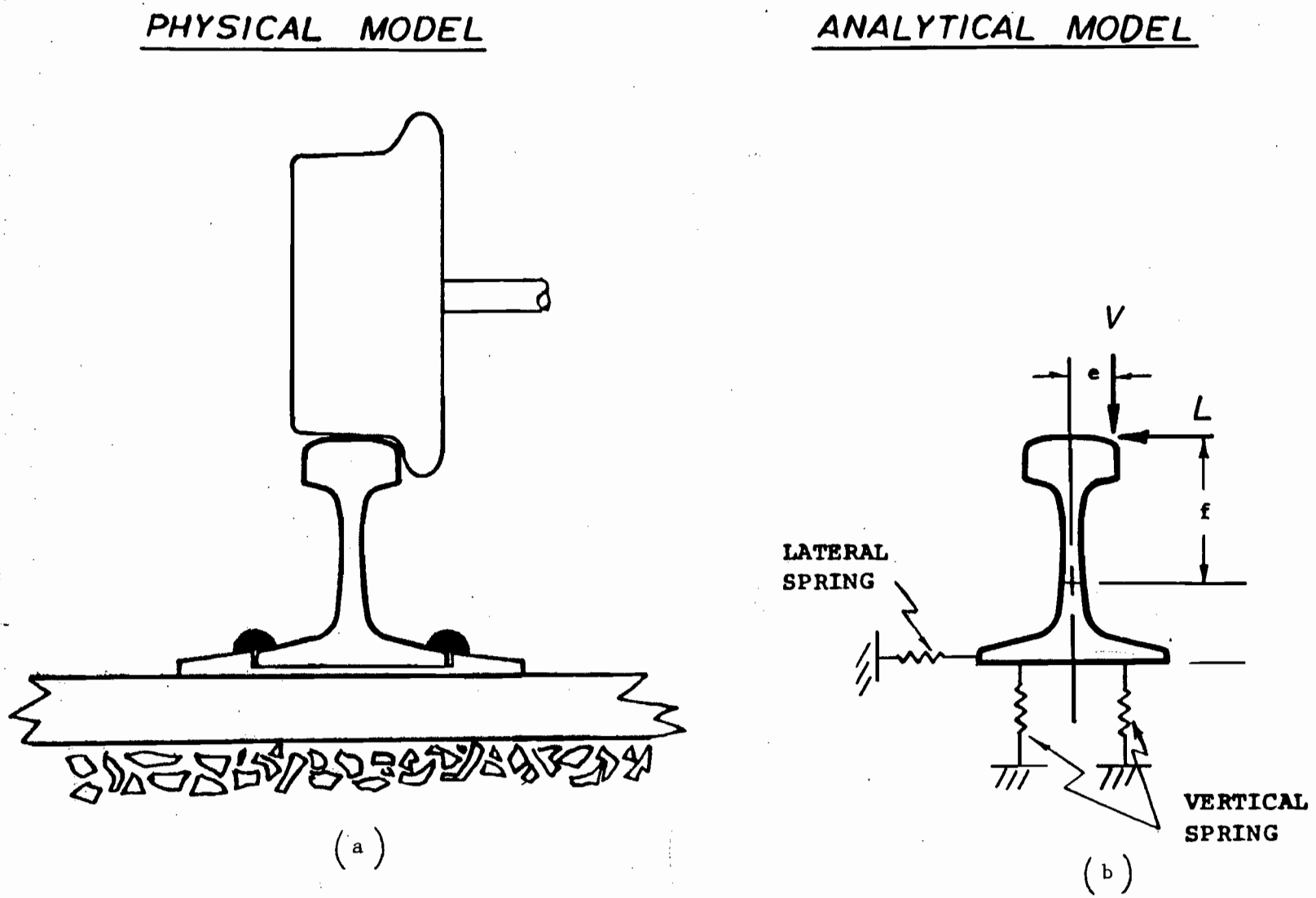

FIG. 2.3 - PHYSICAL VERSUS ANALYTICAL MODEL

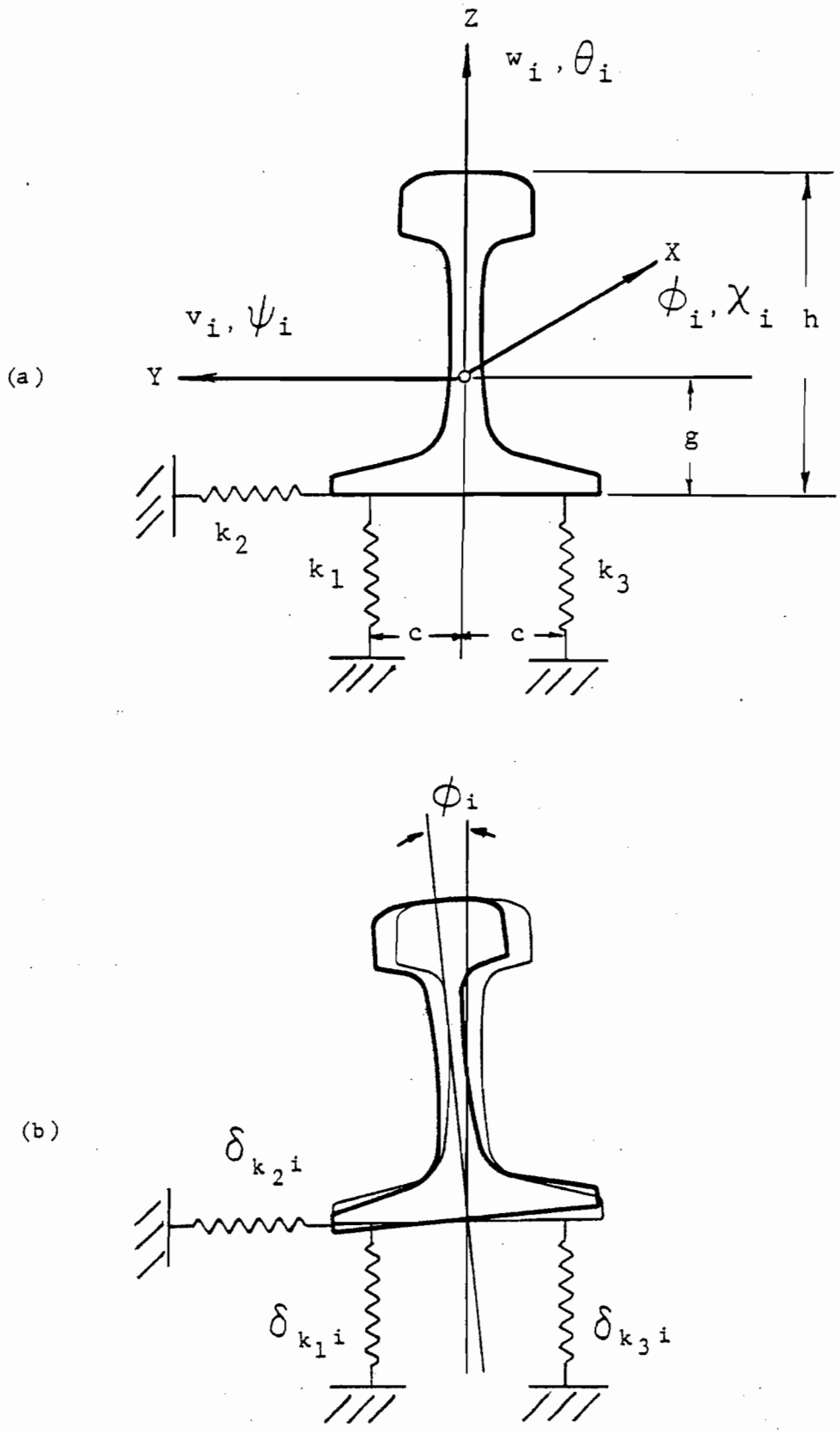

FIG. 2.4 - COORDINATE SYSTEM

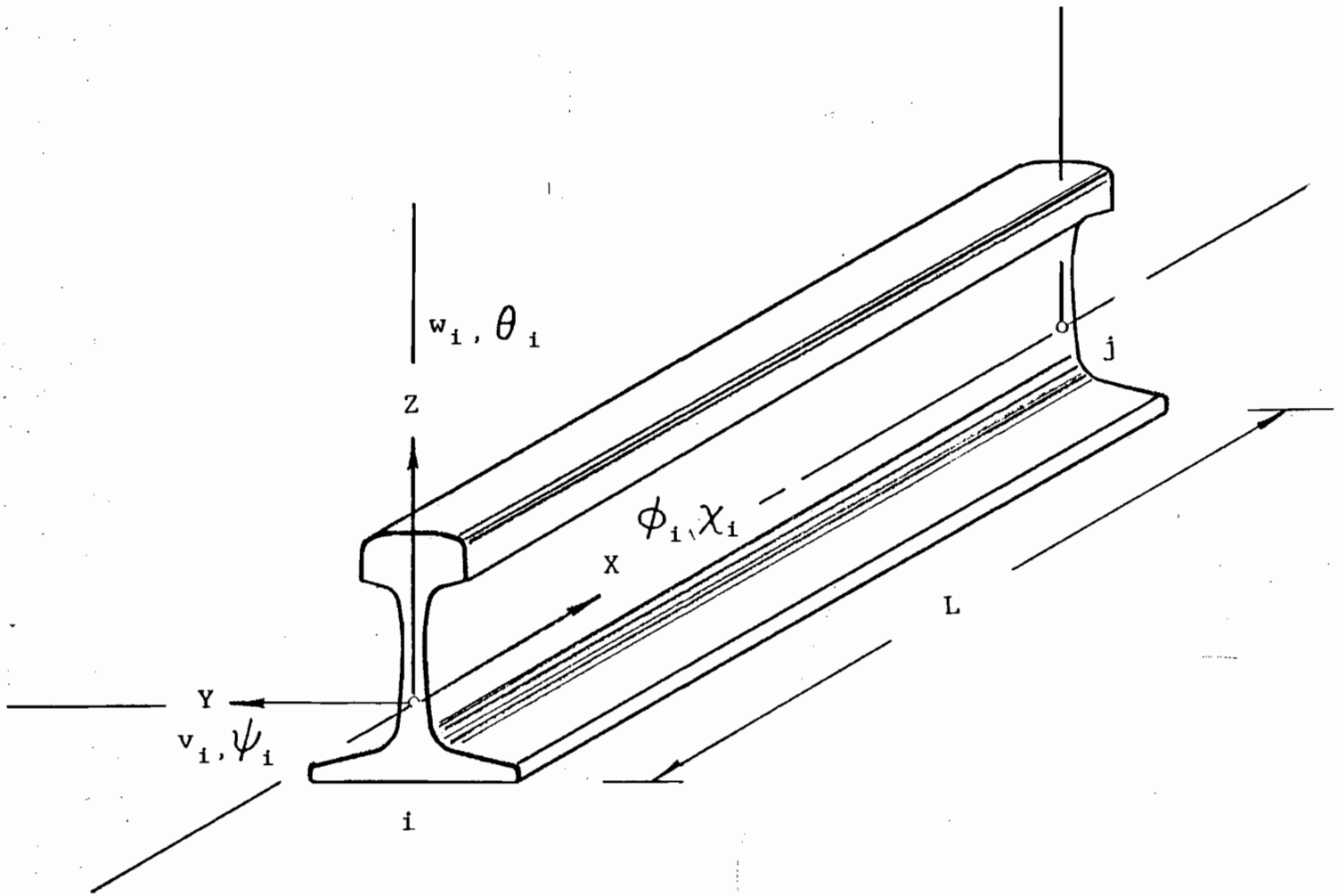

FIG. 2.5 - BEAM ELEMENT

where w = translation in the z direction
v = translation in the y direction
ϕ = rotation in the x direction
θ = rotation in the z direction
ψ = rotation in the y direction
χ = derivative of rotation in x

The components axially along the beam, i.e., displacements between the nodes, can be found if the shape of the displacements are assumed:

$$\{\delta(x)\} = [N(x)]\{\delta_e\}$$

or
$$w(x) = f_1 w_i + f_2 \theta_i + f_3 w_j + f_4 \theta_j$$
$$v(x) = f_1 v_i + f_2 \psi_i + f_3 v_j + f_4 \psi_j$$
$$\phi(x) = f_1 \phi_i + f_2 \chi_i + f_3 \phi_j + f_4 \chi_j$$

where
$$f_1(x) = 1-3\,(x/\ell)^2 + 2\,(x/\ell)^3$$
$$f_2(x) = x(x/\ell-1)^2$$
$$f_3(x) = (x/\ell)^2\,[3-2\,(x/\ell)]$$
$$f_4(x) = x^2/\ell\,(x/\ell-1)$$

The strain energy of the beam element shown in Figure 2.5, as given by Bleich [13], can be written as

$$U = 1/2 \int_o^\ell [EI_y \left(\frac{d^2w}{dx^2}\right)^2 + EI_z \left(\frac{d^2v}{dx^2}\right)^2 + ED \left(\frac{d^2\phi}{dx^2}\right)^2 + GJ \left(\frac{d\phi}{dx}\right)^2] \, dx$$

Using the assumed shape functions and the principle of minimum potential energy, the beam element stiffness matrix can be found:

π_p = potential energy = U - V

$$\pi_p = 1/2 \{\delta_e\}^T [k_e] \{\delta_e\} - \{\delta_e\}^T \{f^{(e)}\}$$

$$\frac{\partial \pi_p}{\partial \{\delta_e\}} = [k_e] \{\delta_e\} - \{f^{(e)}\} = o$$

Evaluating terms in the element stiffness matrix $[k_e]$ requires integrating the derivatives of the assumed shape functions. Numerical integration techniques were applied in order to compute the element stiffness matrices. In particular, Gauss Legendre Quadrature was used in integrating the equations describing the element stiffness matrix.

Generally, the one dimensional Gaussian quadrature formula is easily implemented and is described by the following:

$$I_n = \int_{-1}^{+1} \phi(\xi)\, d\xi = \sum_{i=1}^{N} a_i \phi(\xi_i)$$

where a_i = weighting factor
ξ_i = coordinate of i^{th} integration point
N = total number of integration points

In applying Gaussian quadrature, an n-point rule integrates a polynominal of degress 2n-1, or less, exactly. Therefore, in order to integrate a third degree polynomial, exactly, a Gaussian quadrature of at least 2 points must be used. A list of weighting factors and integration points is shown in Table 2,1. The model described in this document employs a 3 point quadrature rule.

It should be noted that Gaussian quadrature required that the integration be performed over equal intervals; that is, the limits of integration are set from -1 to +1. Therefore, a transformation of co-ordinates is necessary when carrying the integration out for an interval between a and b. That is,

$$\int_{-1}^{+1} f(t)\, dt = \int_a^b f(x)\, dx$$

if

$$t = \frac{2x - (a+b)}{b-a} \quad \text{or} \quad x = \frac{(b-a)t + (a+b)}{2}$$

TABLE 2.1 - GAUSSIAN QUADRATURE

$$\int_{-1}^{+1} \phi(\xi)\, d\xi = \sum_{i=n}^{n} a_i\, \phi(\xi_i)$$

n	i	ξ_i	a_i
1	1	0	2
2	1	$+1/\sqrt{3}$	1
	2	$-1/\sqrt{3}$	1
3	1	0	8/9
	2	$+\sqrt{3/5}$	5/9
	3	$-\sqrt{3/5}$	5/9

2.2.2 Global Stiffness Matrix

In the finite element method, external forces applied to a structure are related to the displacements of the nodal points of each element by a composite matrix of every element in the structure. This composite matrix, called the global stiffness matrix, [K], is computed using the individual beam element stiffness matrices. The "assembly" of the element stiffnesses can be described by the equation

$$[k_{ij}] = \sum_{n=1}^{N} [k_{e_{ij}}^{(n)}]$$

where N = total number of elements. For systems involving a large number of elements, the global stiffness matrix can, indeed, become very large. In the finite element model described in this document each element consists of two nodes which exhibit 6 degrees of freedom. Therefore, the element stiffness matrix, $[k_e]$, is described by a 12 x 12 array. If, for example, a prescribed problem involved 10 ties (i.e., 10 nodes or 9 elements) the global stiffness matrix would be a 108 x 108 array. An array of this size would require over 10,000 terms to describe the global stiffness.

However, a major concern in the application of the finite element method is efficiency. Rather than storing [K] as a two dimensional array it may be worthwhile to store [K] as a one dimensional array. Such a tactic would be successful in reducing core space, if the banded and symmetric properties of the global stiffness matrix are taken advantage of. A discussion of this scheme may be found in Reference 14.

One of the features of the model described here is that the global stiffness matrix also considers the effects of the springs which are attached at the railbase. The spring stiffnesses, however, are functions of the nodal displacements.

At the i^{th} node the deflections of the springs are related to the nodal displacements at that node by (see Figure 2.4b):

$$\delta k_{1i} = w_i - c\phi_i$$

$$\delta k_{2i} = -v_i + g\phi_i$$

$$\delta k_{3i} = w_i + c\phi_i$$

where c = distance between vertical springs (generally approximate to half the width of the railbase

g = distance from the shear center to the base of the rail.

Using these spring deflections, an expression for the potential energy due to the spring deflections at the i^{th} node can be written:

$$V = 1/2\ k_1\ \delta k_1^2 + 1/2\ k_2\ \delta k_2^2 + 1/2\ k\ \delta k_3^2$$

$$= 1/2\ [(k_1 + k_3)\ w^2 + k_2\ v^2 + (c^2\ \{k_1 + k_3\} + k_2\ g^2)\ \phi^2]$$

$$- gk_2\ v\phi + c\ (k_3 - k_1)\ \phi w$$

The equivalent spring stiffnesses are then allocated to the global stiffness matrix.

The springs, however, are considered to be nonlinear (piecewise linear, specifically) when described on displacement versus load curves. Results of component laboratory tests coupled with estimates suggested by linear track models [11] provided the basis for selecting the detailed characteristics of the support springs. To similify the approach, time dependent and frictional resistances are represented by equivalent elastic elements. The selection of load versus deflection behavior of the component resistances is discussed in a later section of this document. These component stiffnesses are based on observations and results of a series of tests performed to examine such resistance behavior. These tests are discussed in Section 3.1.

3. EXPERIMENTAL DATA

To address the deficiency in available data, a sequence of tests was conducted for the Transportation Systems Center by Battelle's Columbus Laboratories in the summer of 1980. These tests, performed in both the laboratory and field, consisted of two parts.

The initial phase focused on the investigation of the response of rail fastener components. Specifically, these component tests were performed to examine spike pullout resistance and tie plate resistance.

The second phase of the test program was a series of field measurements intended to characterize the lateral capacity of track typical of low speed (Class 1 or Class 2) FRA Track Classifications.

3.1 Component Tests

The component tests can be categorized into 2 groups:

1. Spike Pullout Resistance Tests
2. Tie Plate Resistance Tests.

These tests are shown schematically in Figure 3.1. In order to perform these tests two special devices, the Spike Pullout Resistance Device (SPRD) and the Tie Plate Lateral Resistance Device (TPLRD) were designed and built by Battelle. These devices, shown in Figures 3.2 and 3.3, are of light weight and can be used in the field as well as in the lab. Spike vertical force versus displacement and tie plate lateral force versus displacement are measured with these instruments.

The laboratory testing objectives were to develop and demonstrate measurement techniques and to obtain rail restraint data for wood ties. These measurement techniques were then used in the field component tests. The objectives of the field testing were to obtain measurements of spike pullout resistance and tie plate lateral resistance at several locations along the track and to evaluate the data to determine the influencing factors of component resistance characteristics. The influence of tie-spike conditions (i.e.,

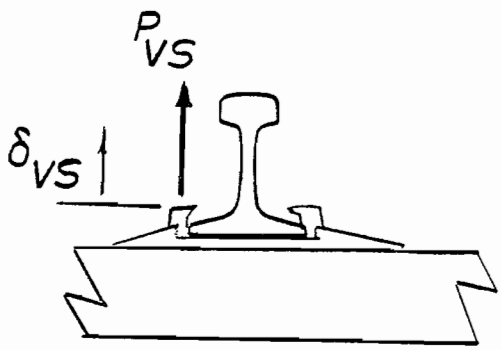

a) Spike Pullout Resistance Test

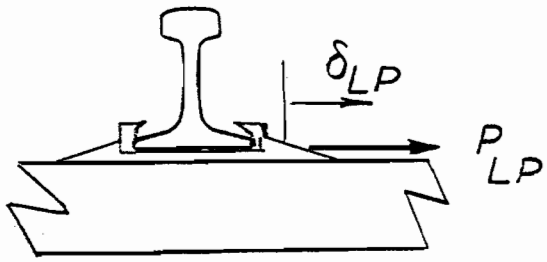

b) Tie Plate Lateral Resistance Test

FIG. 3.1 - SCHEMATIC DIAGRAMS OF SPIKE PULLOUT AND TIE PLATE LATERAL RESISTANCE TESTS

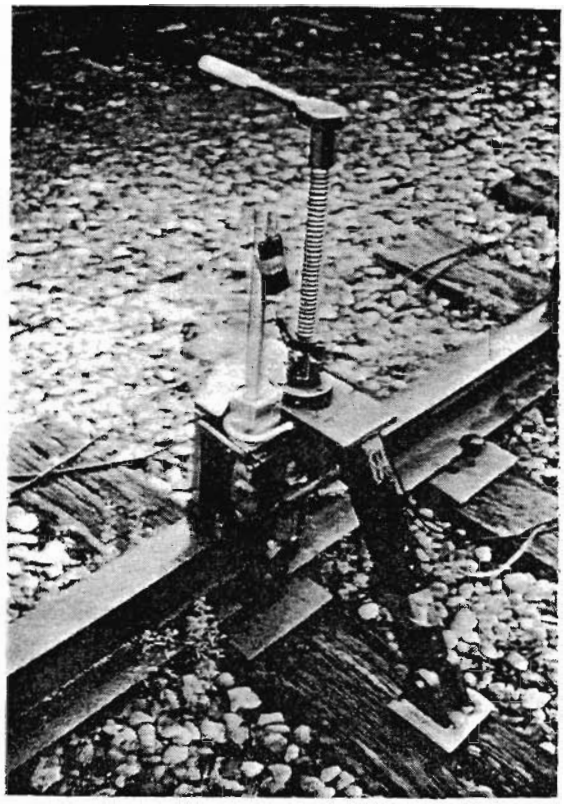

FIGURE 3.2 - SPIKE PULLOUT RESISTANCE DEVICE

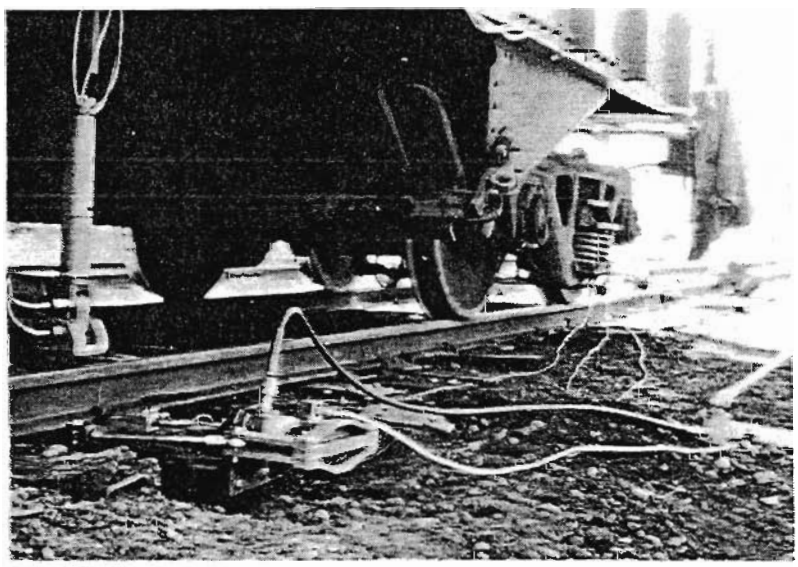

FIGURE 3.3 - TIE PLATE LATERAL RESISTANCE DEVICE

new versus used), spiking pattern, and vertical preload were examined during the component tests.

Detailed descriptions of these tests and of the Spike Pullout Resistance and Tie Plate Lateral Resistance Devices can be found in References 15 and 16.

3.1.1 Spike Pullout Resistance Test

Spike Pullout Resistances were measured in both the field and laboratory for tie conditions ranging from "poor" to "good." A typical result of the spike pullout test is shown in Figure 3.4. The force required to move the spike a finite distance out of the tie, F_{MAX}, declines as more of the spike protrudes (i.e., forms a gap above the railbase). As discussed by Kish, Dzwonczyk, and Jeong [17], the magnitude of F_{MAX} or the amount of force necessary for spike pullout is strongly dependent on the tie and spike conditions. For a badly worn or damanged tie, for example, a spike may be lifted out by hand.

Figure 3.5 compares laboratory spike pullout results for new, good, and poor tie conditions. As can be seen, the general shapes of these curves are similar. The initial slope of the load versus deflection curves increases nearly linearly with displacement to a maximum breakout value, at which point the spike slips upward about 0.1 to 0.2 inches. This slope up to the breakout point decreases with decreasing tie conditions for the examples shown. The force generally decreases with increasing deflection above that for the initial breakout event. This region represents successive breakout events. This behavior is most apparent in the curve for new tie examples and is more subtle for the good and poor tie cases.

These curves can therefore be approximated by a bilinear relationship where an increasing linear region is followed by a decreasing region. The slopes of these regions would be dependent on the tie condition. Figure 3.6 shows such approximations for good and poor tie conditions.

3.1.2 Tie Plate Lateral Resistance Test

Tie Plate Lateral Resistance Tests were also performed in both the field and laboratory. In the lab, however, a surrogate rail segment was used to

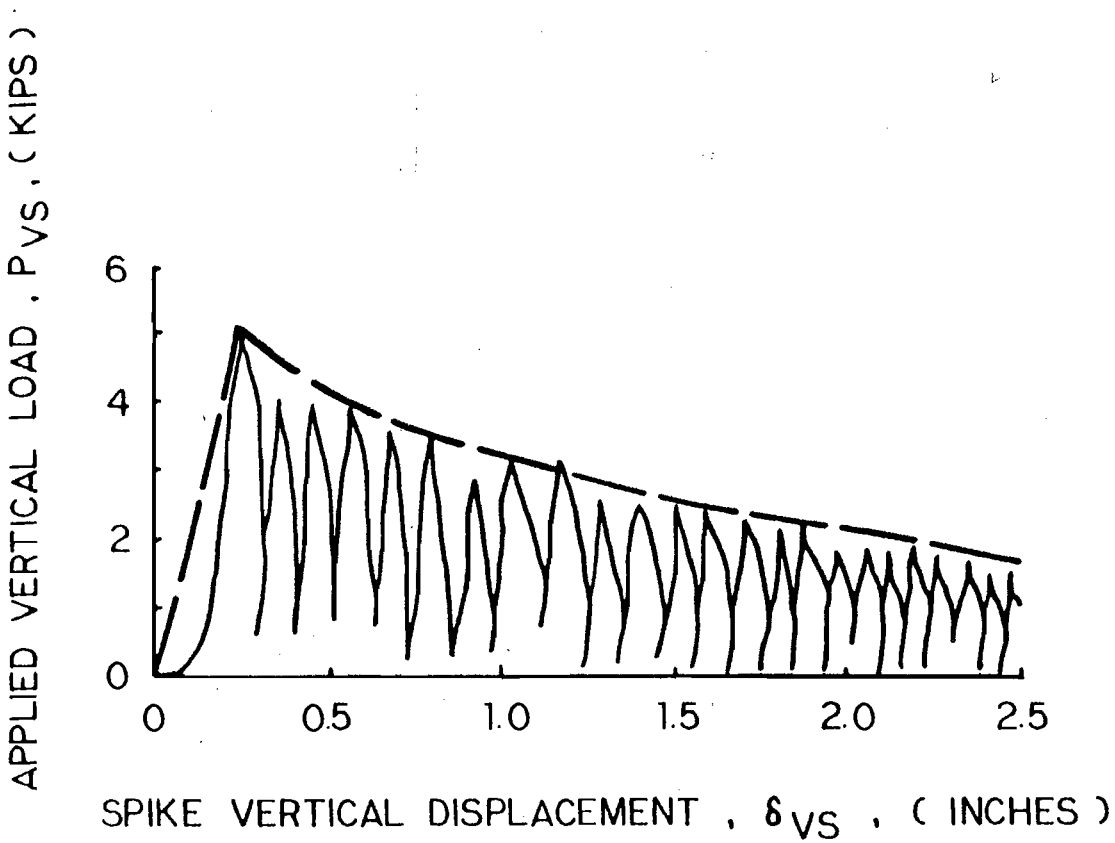

FIG. 3.4 - TYPICAL SPIKE PULLOUT RESISTANCE CHARACTERISTICS FOR A NEW SPIKE/NEW TIE CONFIGURATION

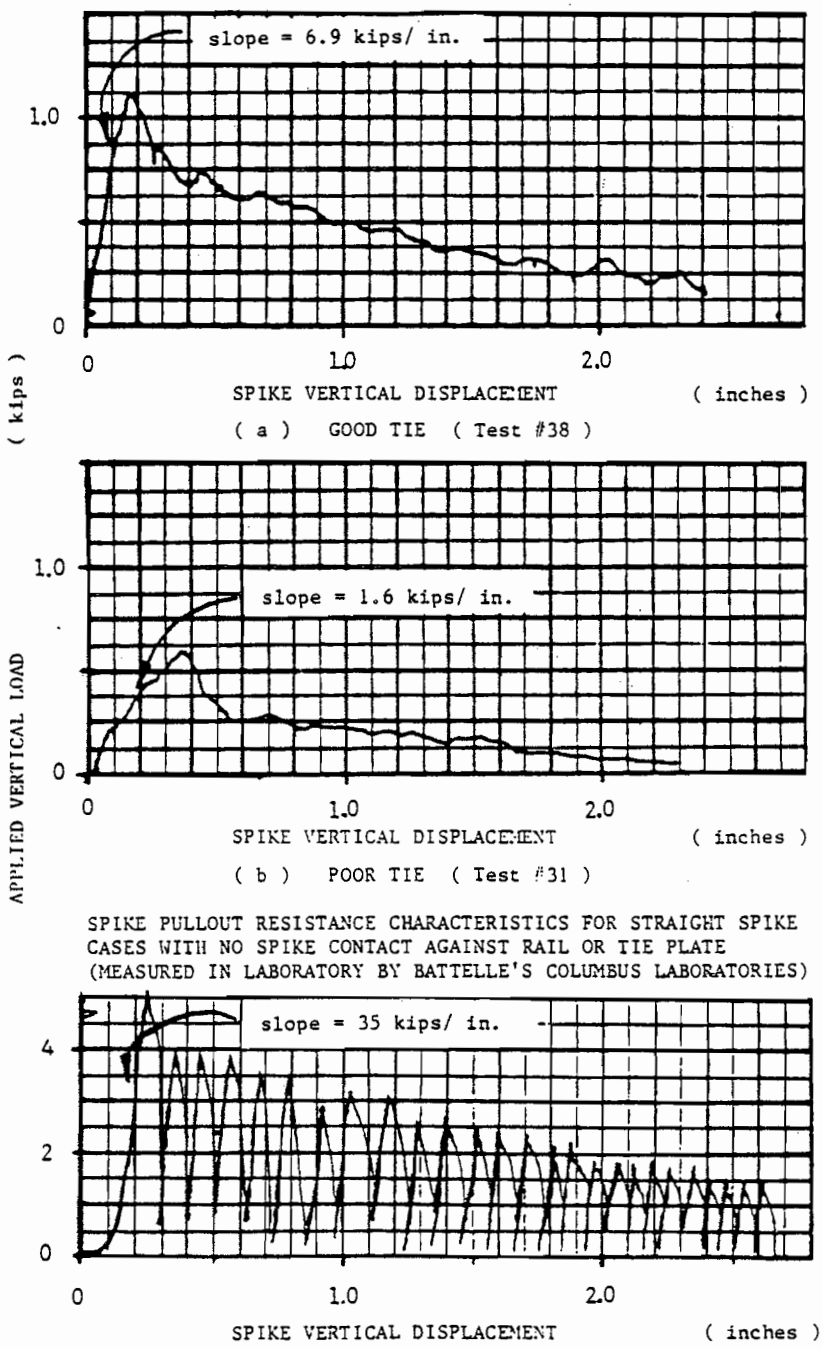

FIG. 3.5 - TYPICAL SPIKE PULLOUT RESPONSES

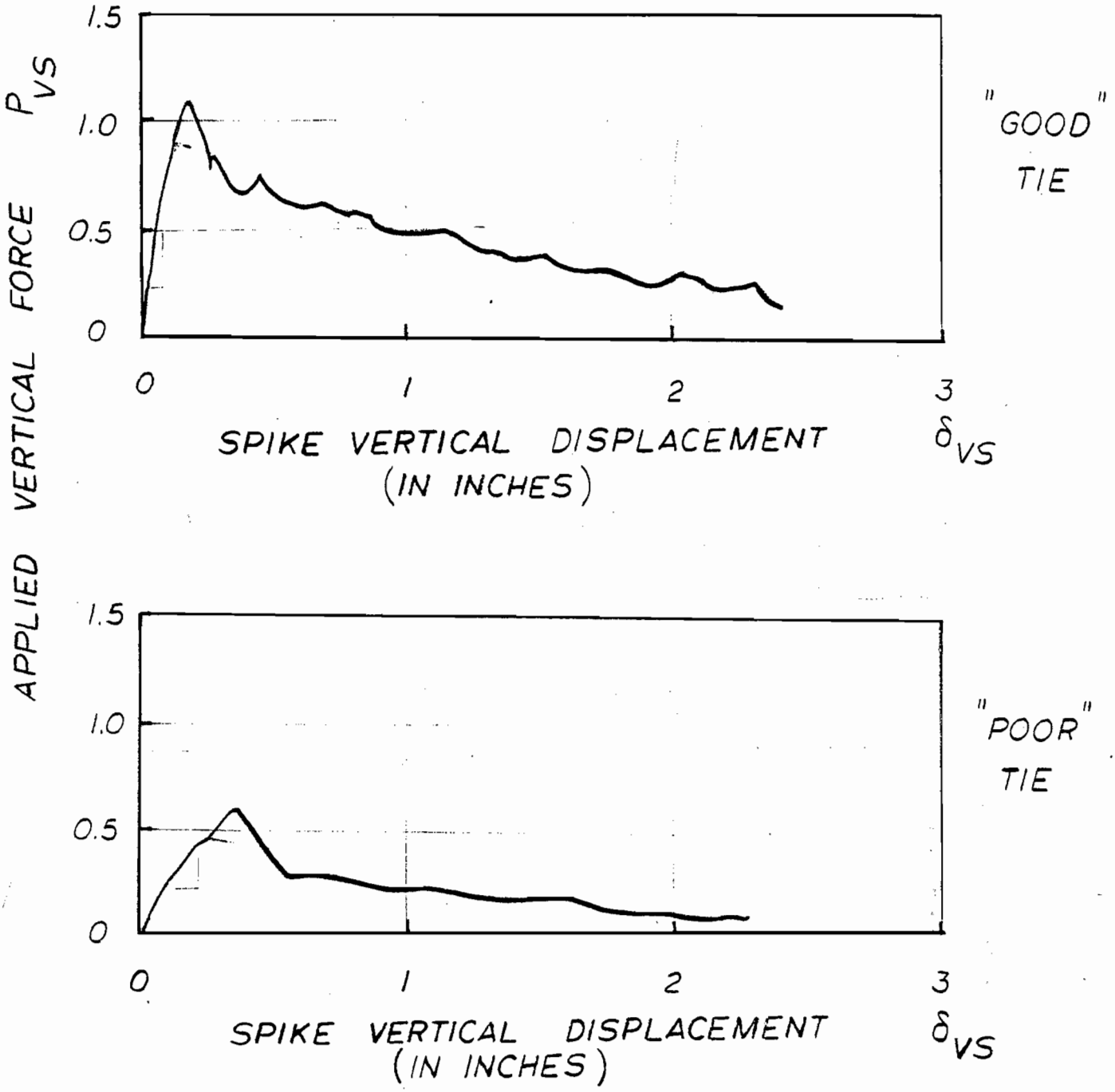

FIG. 3.6 - COMPARISON OF SPIKE PULLOUT RESISTANCES FOR "GOOD" AND "POOR" TIES

test the tie plate resistance. In the field the tie plates of the two adjacent ties in either direction of the test tie were removed. In both field and lab tests the vertical load and tie condition were varied.

A comparison of the field and lab results is shown in Figure 3.7. As shown, there appears to be reasonable agreement between the two tests for varying degrees of conditions (i.e., new and used tie conditions). From these curves of load versus deflection three classes or groups of resistances can be described: low, medium, and high.

The "low" resistance class generally appears to be linear on the force versus displacement curve with a slope of 6-8 kips per inch. This behavior may be caused by a combination of tie plate sliding and cutting with little or no lateral resistance provided by the spikes.

The "medium" class typically appears to be bilinear. The first region exists over the first 0.25 inches of the tie plate displacement while the second region is a nearly constant line of force. This first portion may be the result of combined effects of tie plate cutting and spike bending. The second portion may result from primarily spike rigid body motion which in turn may be caused by yielding of the wood around the spikes.

Finally the "high" resistance class consists of successive high and low stiffness regions. This class of resistance generally applies to new or excellent tie conditions. The probable cause of the behavior of this class may be attributed to participation of one or two line spikes in combined bending and rigid body deflections and tie plate sliding along with no tie plate cutting.

Figure 3.8 shows the effect of vertical preload on the laboratory and field tests. Assuming that half of the vertical load applied to the railhead in the field test is applied to the tie plate, the field and laboratory tests appear to be reasonably consistent under similar conditions. For the field test results three cases are shown in the figure: case 1 is a good tie with the spikes-tie plates of adjacent ties not removed; case 2 is also a good tie but the two adjacent spike/plate systems on each side of the test tie were

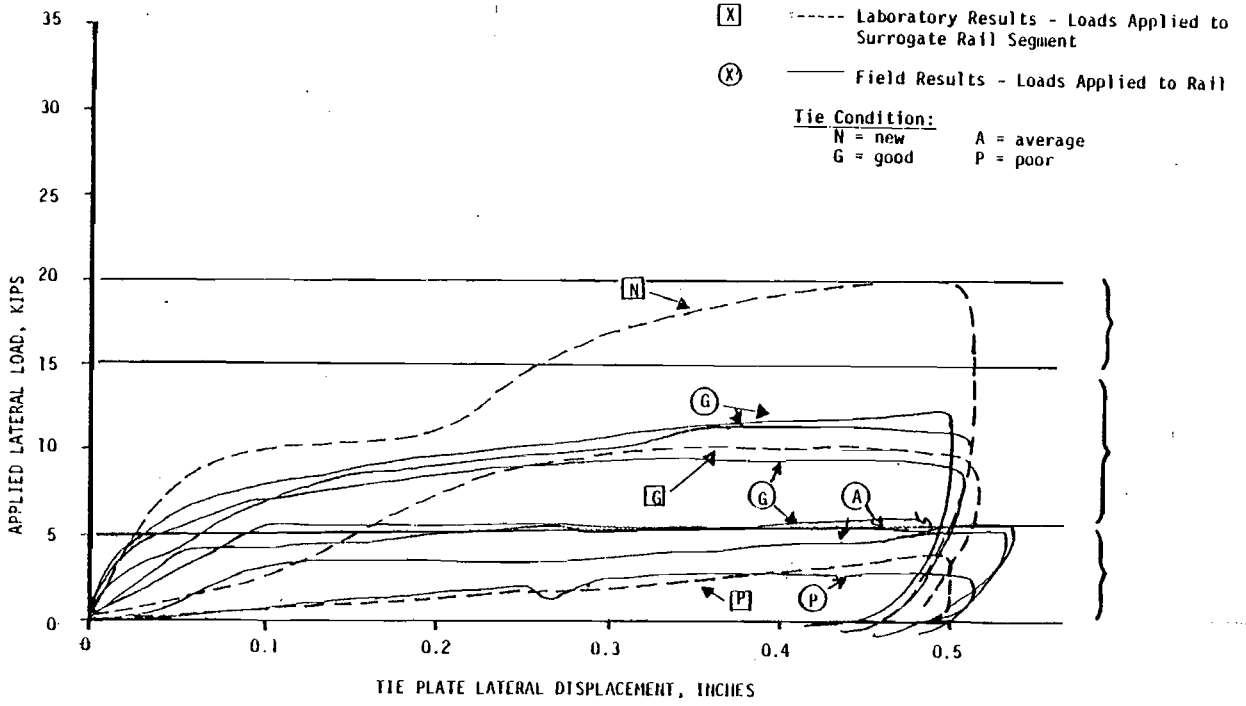

FIG. 3.7 - COMPARISON OF FIELD AND LABORATORY RESULTS OF TIE PLATE LATERAL RESISTANCE TESTS CONDUCTED ON TIES IN SEVERAL CONDITIONS (NO VERTICAL PRELOAD)

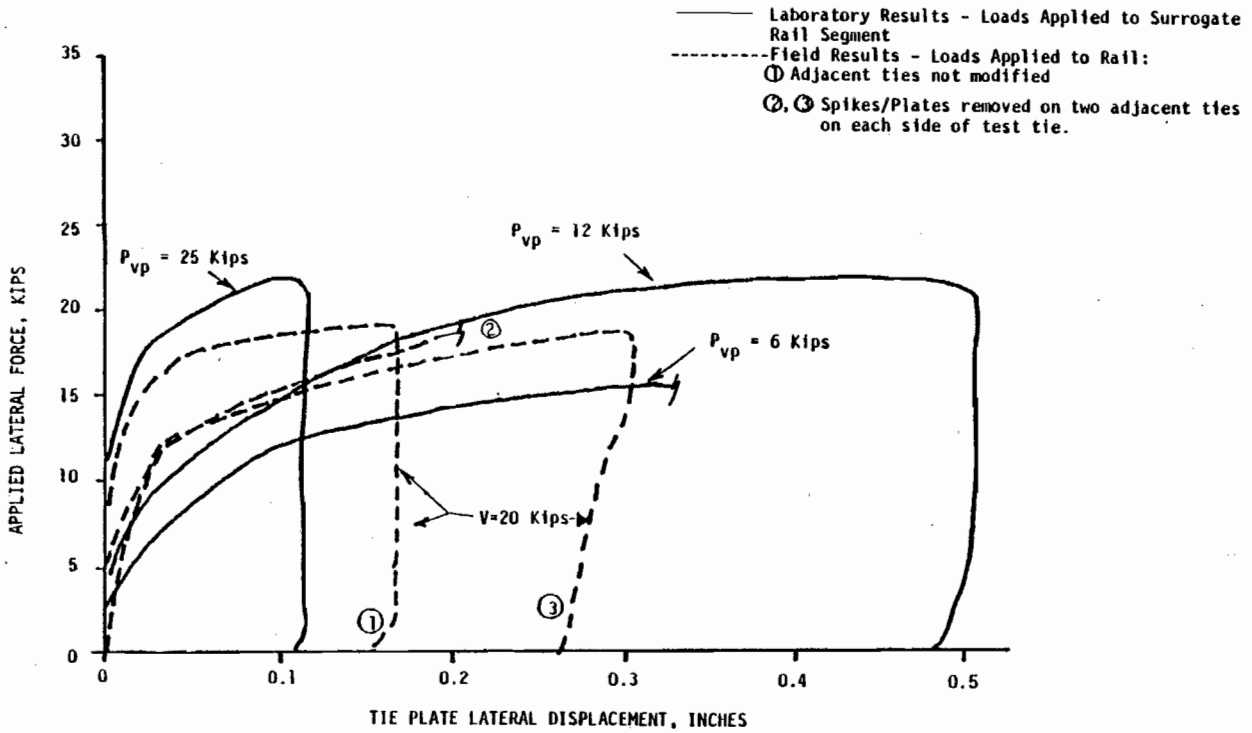

FIG. 3.8 - COMPARISON OF FIELD AND LABORATORY RESULTS OF TIE PLATE LATERAL RESISTANCE TESTS

removed, and case 3 is the same as case 2 but with a poor tie.

The shapes of these curves generally seem to be similar. For the field test case 2 there appears to be a bilinear function of load versus tie plate lateral displacement. The first region consists of an initial slope up to 0.3 inches of high stiffness and the second region is a level of low stiffness. Cases 1 and 3 of the field test shown also show this behavior but with an initial breakout level, i.e., offset starting at 5 to 8 kips. Thus for these two cases a trilinear function may be apparent to approximate the tie plate lateral resistance where the first region may be attributed to a frictional force. The presence of a vertical preload alters the behavior which may be explained by a normal force applied to the tie plate as it slides. Figure 3.9 shows a piecewise linear approximation of a tie plate lateral displacement, accounting for a frictional term.

In addition to lateral load resistance measurements of the tie plate, a series of tests were made in the field, to determine the force-deflection curves for vertically applied loads. The basic setup of these vertical tie plate modulus measurements is shown in Figure 3.10a. As can be seen a pair of 0.5 inch range DCDT's were installed on the rail at diagonally opposite corners of the tie plate. Typical results for "good" and "bad" tie conditions are shown in Figure 3.10b. These plots represent an internal track stiffness which is primarily controlled by local deformations of wood under direct contact from the rail on either side of the submerged tie plate. The compression of the tie due to bearing pressure from the whole tie plate is another controlling factor. From the results it can be seen that for good tie conditions the response is nearly linear but for poor conditions the response is nonlinear. It should be noted that the input load is essentially a rail base or tie plate load not a wheel load since the adjacent ties for three ties in both directions of the test tie were removed.

3.2 Field Tests

The second phase of testing was a series of field tests performed with the following objectives:

- o to obtain large displacement load-deflection data for "minimally" adequate in-service track

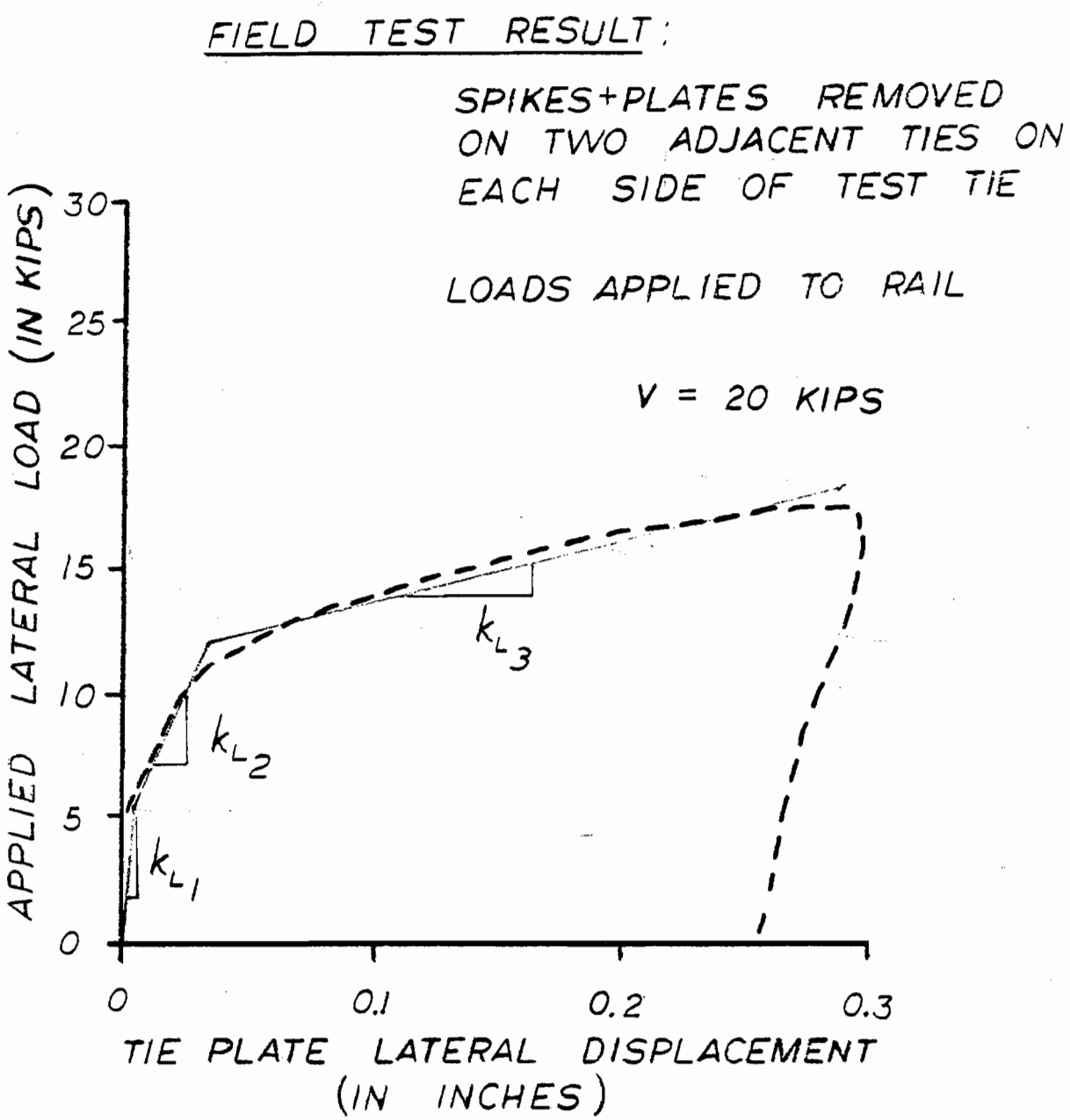

FIG. 3.9 - PIECEWISE LINEAR REPRESENTATION OF THE TIE PLATE LATERAL DISPLACEMENT VERSUS LATERAL LOAD CURVE

(a)

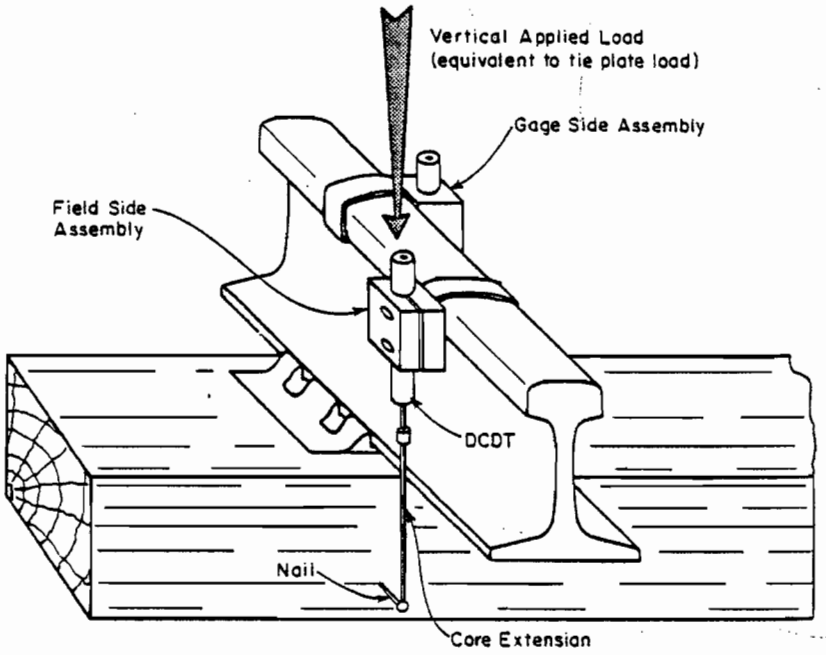

(b)

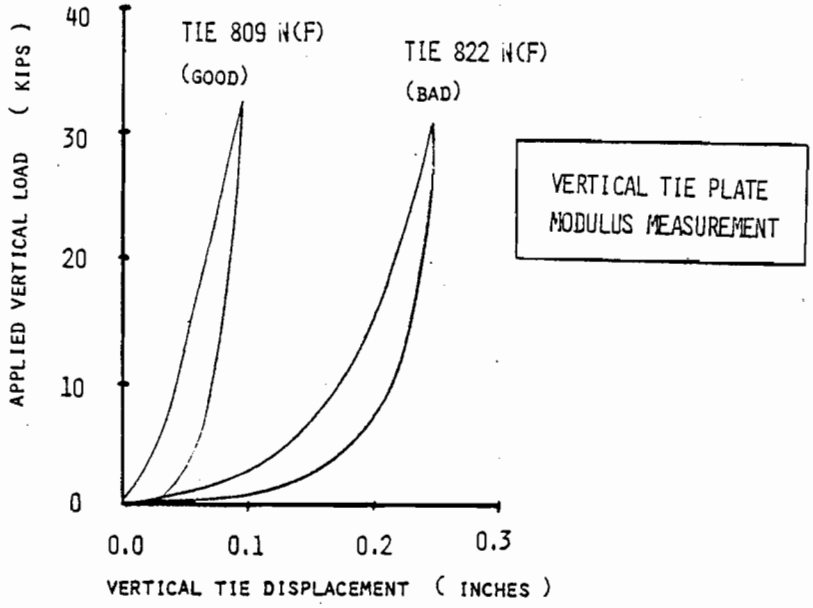

FIG. 3.10 - VERTICAL TIE PLATE MODULUS MEASUREMENT

- o to establish a statistical range of load-deflection characteristics
- o to obtain component data on spike pullout and tie resistance required for further analysis.

To meet these objectives acceptable sites for these tests were required to have the following characteristics:

- o a uniform mixture of "good" versus "bad" ties
- o enough variability in tie-tie plate-spiking conditions to afford a good sample of
  - i. defective ties
  - ii. missing spikes and plates
  - iii. 3 or 4 defective ties in a row
  - iv. 1 or 2 defective ties flanked by good ties.
- o rail size typical of most low speed track
- o accessible territory-availability

In the context of this report, a defective tie is used to refer to a tie which is deteriorated beyond generally accepted industry standards. A cross-tie was considered to be "defective" when it was:

1) broken through;
2) split or otherwise impaired so that it will not hold spikes or will allow the ballast to work through;
3) so deteriorated that the tie plate or rail base can move laterally more than 1/2" relative to the crosstie;
4) not spiked with at least 1 field and 1 gauge spike per rail per tie.

The specific site chosen was the Hocking Division, Pomeroy Subdivision of the Chessie System, near Logan, Ohio, between mile-posts 55 and 57 near Union Furnace. The characteristics of this site are listed in Table 3.1.

A specially designed track loading fixture (TLF) mounted on the underframe of a loaded hopper car, shown in Figure 3.11, was used to provide vertical and lateral loading to the rails. The loading fixture was hydraulically powered with a capacity of 50 kips vertical and lateral load. The actual load transfer to the rails was accomplished through a standard 36 inch diameter AAR wheel segment. Actual single point wheel-rail contact is, therefore, simulated very closely by the TLF as the rail deforms. Further description of this

TABLE 3.1 TEST SITE DESCRIPTION

GENERAL CONDITION:	OUT OF SERVICE FOR 6 MONTHS PREVIOUS SPEED LIMIT: 25 MPH (TYPICAL SPEEDS : 10 MPH) TANGENT TRACK MILD (.3%) GRADE EXCELLENT GAUGE AND ALIGNMENT
RAIL:	100 LB/YD NOT BADLY WORN
TIES:	WOOD MIXTURE OF "GOOD" AND "BAD" SPACING OF 20"- 22"
PLATES & SPIKES:	SINGLE SHOULDERED TIE PLATE TWO LINE SPIKES/PLATE
BALLAST:	CINDER/GRAVEL

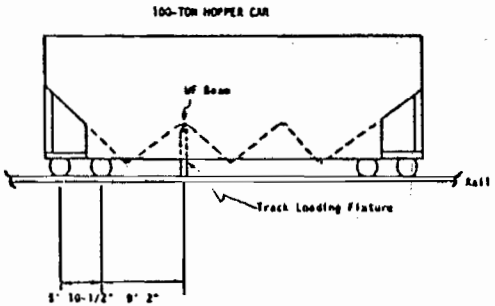

TEST SET-UP FOR RAIL RESTRAINT MEASUREMENTS

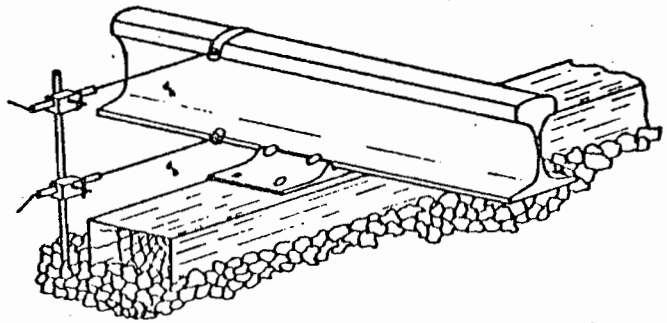

DISPLACEMENT FIXTURE FOR ONE RAIL (SAME FOR OPPOSITE RAIL)

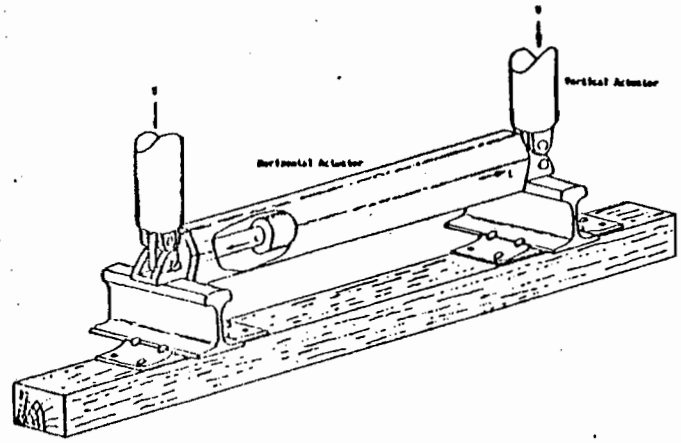

BASIC LAYOUT OF TRACK LOADING FIXTURE

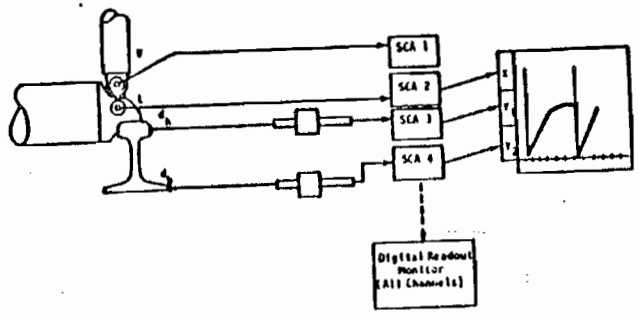

MEASUREMENT SYSTEM FOR ONE RAIL (HALF OF TOTAL SYSTEM)

FIGURE 3.11- TEST SETUP FOR RAIL RESTRAINT MEASUREMENTS

device can be found in Reference 15. Figure 3.11 also shows schematically the displacement transducer and recording arrangement. Lateral displacements of the rails were measured at the rail head and rail base with DCDT's capable of measuring up to 3 inches of rail head displacement and 2.5 inches of rail base displacement.

To insure a reasonable sample, as well as variety and variation in rail restraint conditions, the sequence of tests indicated by the matrix in Table 3.2 was conducted. Generally, the test procedure ran as follows:

- o position hopper car-load jack and mount displacement transducers
- o record initial gauge and transducer rod separation
- o apply vertical preload and record lateral load versus railhead and railbase displacements
- o unload lateral load then vertical
- o record final gauge.

The most conspicuous result was a large variation in railhead displacement response depending on the local tie and fastener configuration. Figure 3.12 shows the substantial difference in load capacity at a given head deflection of typically "good" and "bad" test sites. For instance in this case the bad tie was found to be weaker with a 32 percent reduction of lateral load at 1 inch lateral deflection of the railhead. In general, this behavior of load versus railhead deflection appears to be bilinear for the strong tie and non-linear for the weak tie. The latter behavior was found to be the more typical of all the tested ties. Figure 3.13 shows the railbase deflections and the railhead deflections with lateral load for the same two test ties. It can be seen that the difference between railhead and railbase deflection increases as the applied lateral load increases. Again, the influence of tie condition can be seen by the reduction in strength for both the railhead and railbase deflections.

Another result of the test can be illustrated through Figure 3.14 in that the presence of vertical load increases or strengthens the resistance against gauge widening. This strengthening effect of vertical load as well as the

TABLE 3.2 RAIL RESTRAINT MEASUREMENT TEST MATRIX

TEST SERIES NUMBER	VERTICAL PRELOAD, V (KIPS)	RAIL HEAD DISPLACEMENT, LIMIT (INCHES)	NUMBER OF LATERAL LOAD CYCLES	NUMBER OF TESTS
1.1	15	3	1	38
1.2	30	3	1	26
2.1	15	1 , 3	2	2
2.2	30	1 , 3	2	2
3.1	5 , 15	1 , 3	2	8
3.2	5 , 30	1 , 3	2	8
4	15, 30, 45	1/2, 1,2	9	4
5.1	15	1	26	2
5.2	30	1	26	2

SPECIAL TESTS:

ADJACENT LOAD INFLUENCE	V = 15, 15, 30
TWO AND THREE MISSING TIES	V = 15
WEAKENED TIES, SPIKES REMOVED	V = 15
WEAKENED JOINT, BOLTS REMOVED	V = 15
VERTICAL TIE PLATE MODULUS	V VS δ_v

COMPONENT TESTS: SPIKE PULLOUT CHARACTERIZATION
TIE PLATE LATERAL RESISTANCE

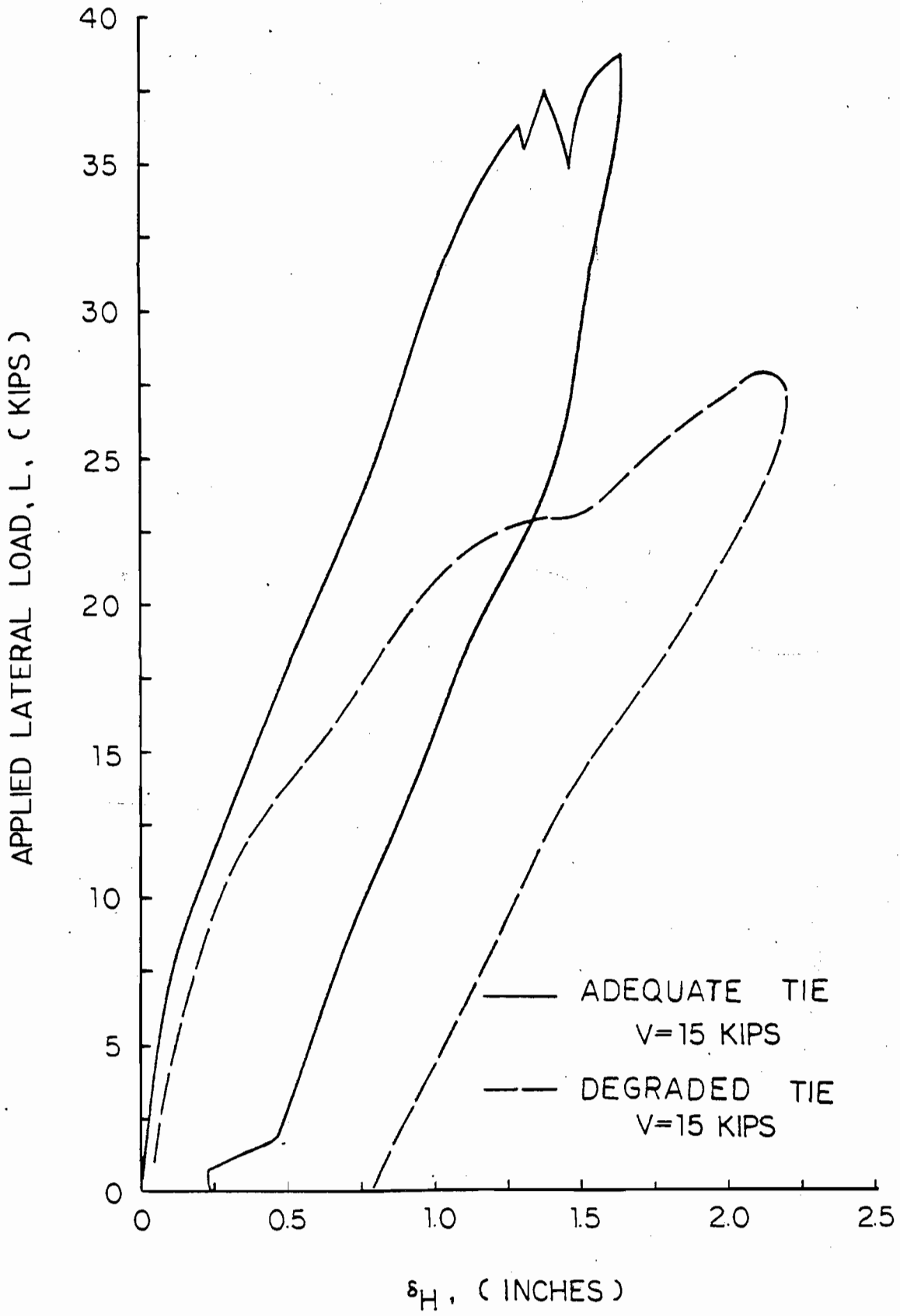

FIG. 3.12 - TYPICAL "STRONG" VERSUS "WORN" LOAD DEFLECTION BEHAVIOR

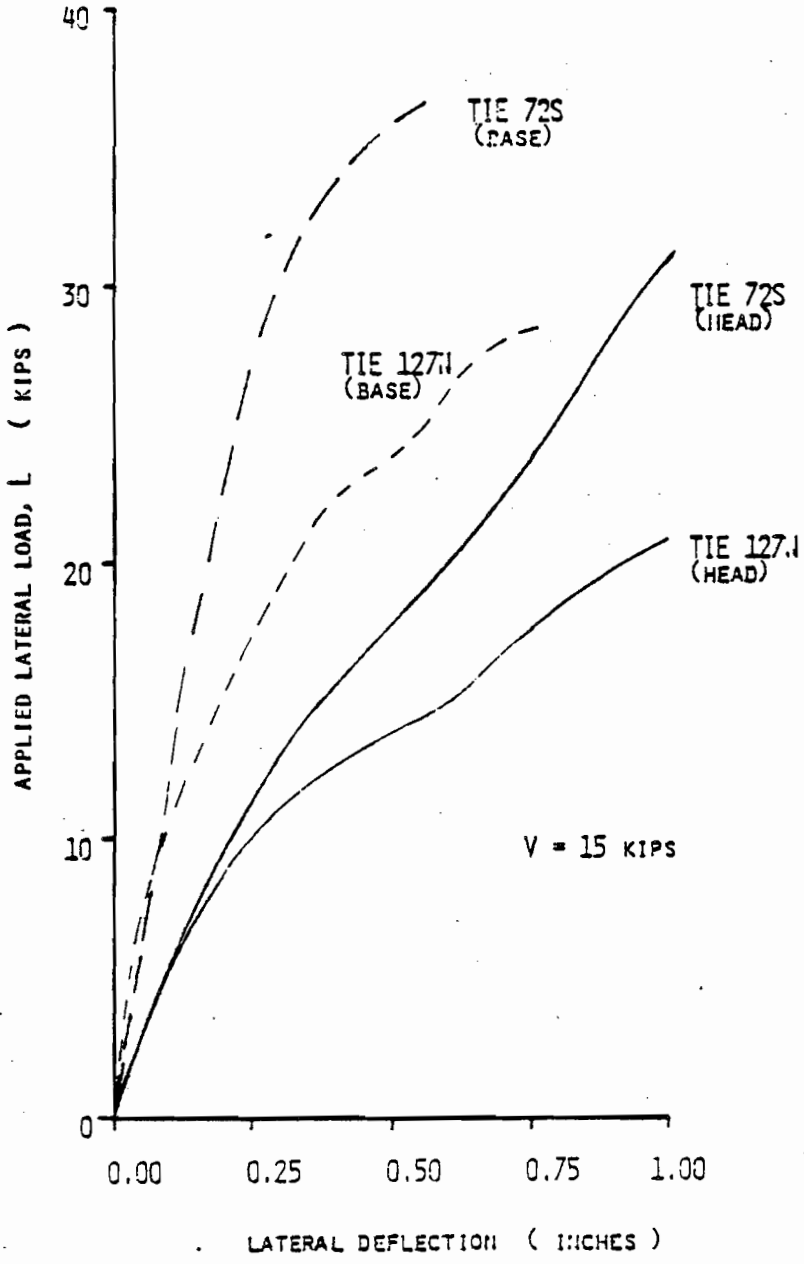

FIG. 3.13 - RAILHEAD AND RAILBASE LATERAL DEFLECTIONS

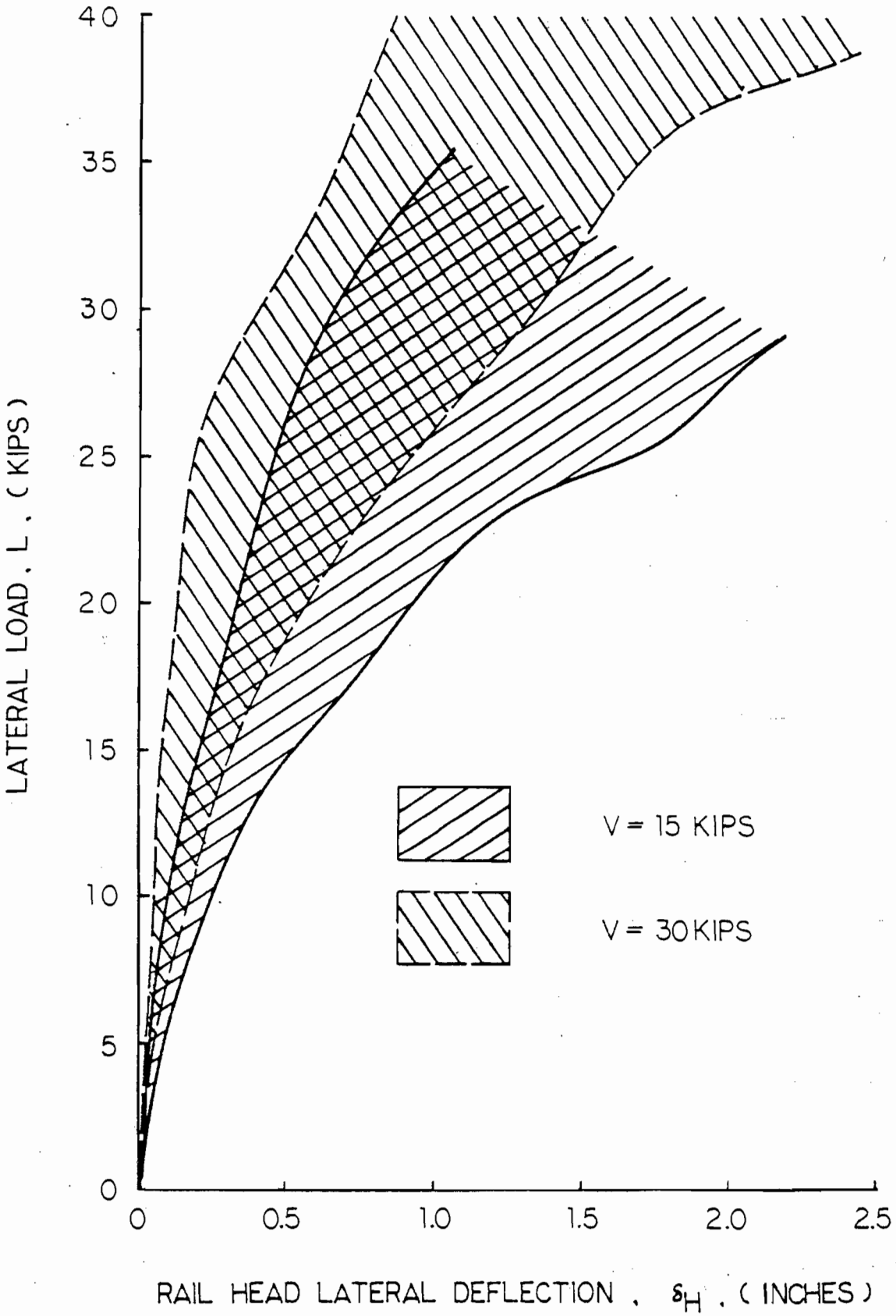

FIG. 3.14 - LATERAL LOAD VERSUS RAILHEAD LATERAL DEFLECTION SUMMARY

range of head displacement can be seen in this figure. For example, at one inch of head deflection the lateral load ranged from roughly 20 to 35 kips with vertical load (approx. 43% reduction) of 15 kips and from 25 to 42 kips when the vertical load was 30 kips (approx. 40% reduction).

In addition, the corresponding displacement responses of the rail base and of the rails on ties near the one being loaded were of significant interest, since they were quite different from those observed in laboratory tests, particularly for the test conditions reported by Choros, Zarembski, and Gitlin [2].

The results of the field tests can be summarized as follows:

- observed failure modes
  - rail rotation with simultaneous rail lateral shift
  - tie plate "submarining" into tie
  - tie crushing, spike bending, spike hole elongation
- rail base displacements
  - 30% to 50% of head displacements for high lateral loads (35 kips)
  - 50% to 70% of head displacements for intermediate lateral loads (25 kips)
  - 70% to 90% of head displacements for low lateral loads (15 kips)
- "Influence zone": 6 to 7 ties for good section and 10 to 12 ties for bad section
- Tie visual inspection-appearance may indicate potentially weak capacity but is inadequate for actual strength capacity assessment.

4. PARAMETRIC STUDIES AND RESULTS

Three elements have been provided in an attempt to examine the phenomena of gauge widening:

1. Field test data
2. Component test data
3. Rail Analytical Model.

Each of these elements was obtained through tasks with specific objectives in mind. For example, the field tests were performed to acquire gauge widening data for typically low speed track. These tests were also intended to complement the component tests and the development of the analytical model. The component tests were performed to examine spike pullout and tie plate lateral resistance characteristics.

Using these three elements a parameter search was performed with the following objectives:

- investigate the key parameters influencing gauge widening
- determine the capacity of low speed track necessary to provide adequate lateral restraint to prevent gauge widening failure.

In performing this parameter identification the results of the component tests are used along with the analytical model to predict the lateral load versus deflection behavior for both the rail head and rail base. These load versus deflection curves are then compared to the appropriate field test results. The parameters of the analytical model are then altered until the predicted load-deflection response is within reasonable agreement with the corresponding field test results. Particular interest in this procedure is given to weakly supported track since track condition is an important factor in establishing a lower bound of support. Initially this parameter search is performed for a vertical load of 15 kips. Once the parameters have been identified at this vertical load level the same parameters are used in predicting load versus deflection behavior for vertical loads of 5 and 30 kips.

An important point to note is that for a vertical load applied at the gauge corner of the rail with no lateral load, the rail head deflection will

be negative; that is, toward the gauge side. As the lateral load is increased the rail head will move toward the field side. However, loads applied at the gauge corner generally occur at extreme cases where the lateral-to-vertical load ratio is relatively high. The results of the parametric studies are presented by extrapolating the lateral load versus rail head deflection curve to the origin from approximately 7.5 to 10 kips.

4.1 Component Stiffness Identification

4.1.1 Selection of Component Stiffness

Parameters for the rail analytical model require the knowledge of the component resistance characteristics. Load versus deflection behavior of spike pullout resistance and tie plate lateral resistance were obtained in these component tests. In order to apply the results of these tests to the analytical model, approximations of the shapes of these load versus deflection curves must be assumed. As pointed out in previous sections, the component test data results exhibit distinguishing points of interest in the load-deflection responses. More specifically such curves can be approximated by piecewise linear increments where the changes in slopes are found at these salient points.

It should be pointed out that the selection of the component stiffness characteristics is based on the field test data. Therefore these stiffnesses are intended to represent support of weak or poorly conditioned track (FRA Class 1).

From both field test and laboratory test data, the lateral stiffness appears to have a softening effect. Initially a beam on elastic foundation model was implemented to examine the location and number of breaking points required to define the lateral stiffness. The specific model that was employed was the one developed by Timoshenko and Langer [10] which allows for the coupled flexure and twist of a rail supported on a continuous, linear and elastic foundation. These calculations involved comparisons between the rail base deflection versus lateral load responses for the continuous foundation model and the field test data for corresponding degrees of track parameters. Through this procedure the first incremental slope and breaking point were found since this region is nearly linear. However, subsequent breaking points

in the nonlinear range were not found as easily. The results of the component tests were used as an aid to estimate and adjust the location of these breaking points. From the component tests, the lateral stiffness appears to be comprised of three regions (see Figure 4.1).

It can be seen that the initial slope, k_{L1}, may be attributed to a friction term where a normal force is present along with a coefficient of friction. This slope is very large, characteristic of dry friction behavior. The intermediate slope is related to the elastic behavior of spike bending while the final slope, k_{L3}, corresponds to a predominantly sliding mode of response. For badly worn ties, the intermediate k_{L2} region, when the tie plate digs or submarines into a tie, is typical of relatively strong track. It should be pointed out that the analysis discovered that these three slopes and the appropriate breaking points are sufficient to define the lateral spring properly. Additional slopes and breaking points do not appear to alter the railbase versus lateral load response greatly. Also, the characterization of the lateral stiffness as a curve with three slopes seems consistent with the component test data. Recall from previous sections that the lateral component tests exhibited bilinear behavior when vertical load was not present and an offset plus bilinear response when vertical load was present. The component stiffnesses after the initial break point were chosen somewhat stiffer (conservative) than the component test values. As a result the effect of rotation must be assumed by the vertical stiffness components.

The selection of the vertical stiffness components must consider two influences: 1) vertical load, and 2) rotational stiffness. The first issue addresses a trend found in the field test results; that is, vertical load strengthens the resistance against gauge widening. The rail deflection versus lateral load behavior is altered for varying vertical loads. Selection of a vertical stiffness that is too low (soft) will spread this vertical load effect while a vertical stiffness that is too high (stiff) will contract the effect. First order estimates of the vertical stiffness components were found to be somewhat low with respect to the available data. Such approximations compensate for the lateral stiffness selection but leaves less room for reduction if large rotation is required at high load levels. The behavior of the vertical stiffness component is based on response observed in the com-

(a)

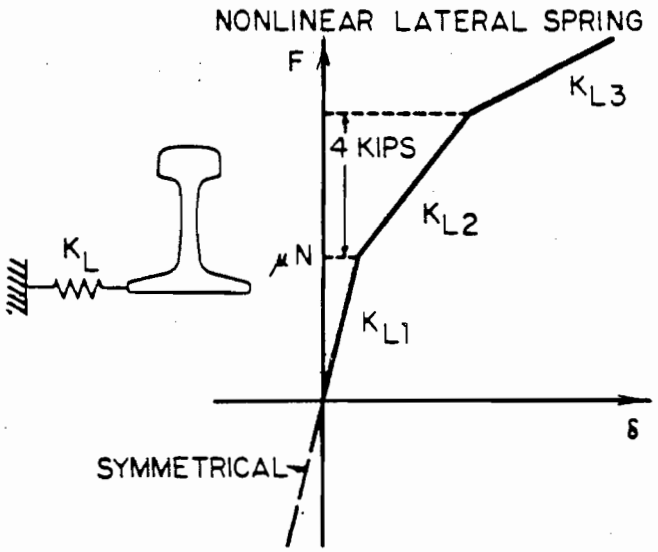

N = VERTICAL FORCE ON TIE PLATE
$\mu = 0.4$

(b)

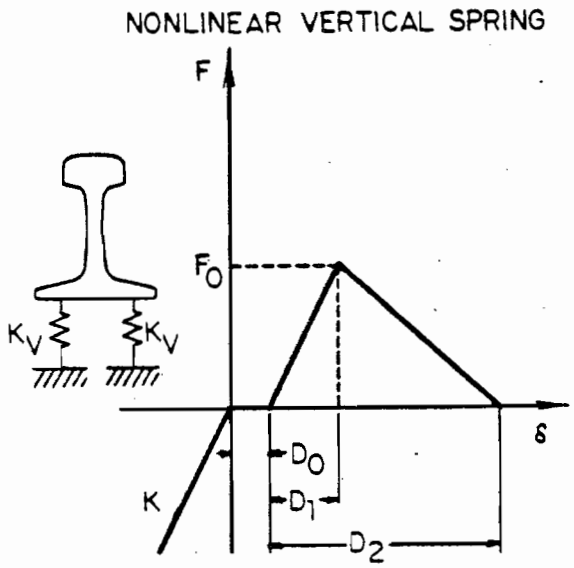

F_0 = PEAK SPIKE PULL OUT FORCE

D_0 = GAP BETWEEN SPIKE HEAD AND RAIL BASE SURFACE

FIG. 4.1 - PIECEWISE LINEAR REPRESENTATIONS OF VERTICAL AND LATERAL STIFFNESS COMPONENTS

ponent resistance tests and the compression response of the vertical tie plate-foundation combination. Referring to Figure 4.1a, the portion of the response curve in the negative quadrant is representative of the response found through the vertical tie plate modulus measurement. The slopes in the positive quadrant represent the general responses found in the spike pullout tests. A gap forming between the spike head and the rail base may result as the spike is pulled upward as the rail rolls repeatedly. Such a loss mechanism may be accounted for in the vertical stiffness characterization. From Figure 4.1b it can be seen that the distance, D_o, will increase if a load as large as F_o is applied. It was discovered through the identification procedure that this gap or loss mechanism is another important parameter in distinguishing between relatively strong and relatively weak track. For instance, rail head versus lateral load curves may exhibit a softening and then a stiffening effect when the gap or loss mechanisms is included while relatively strong lateral stiffness is present. Although strong lateral support is provided it is the vertical stiffness, or this dead band region in particular, that controls the stiffening response.

4.1.2 Variation in Component Characteristics

Component characteristics of varying degrees of stiffness were found through the parameter identification. The field data were used to obtain an overall average lateral load versus railhead reflection response. This mean response characteristic was found by averaging the lateral load levels at different values of constant deflection. Thus load-deflection curves were generated for varying vertical loads. Lower and upper bounds of this data were also established. The calculations of these lower and upper bounds involved averaging responses of a selected set of data. The lower bound test cases seem to be a composite of three degrees of tie condition:

i. degraded
ii. worn, but not excessively deteriorated
iii. 2 or 3 consecutive missing ties.

A summary of lower bound field test cases for a vertical load of 15 kips is shown in Figure 4.2. The composite lower bound for V = 15 kips was found by averaging the two (tie #1077) and three (tie #1067) missing tie cases. In general, the upper and lower bound composite curves are found by averaging the

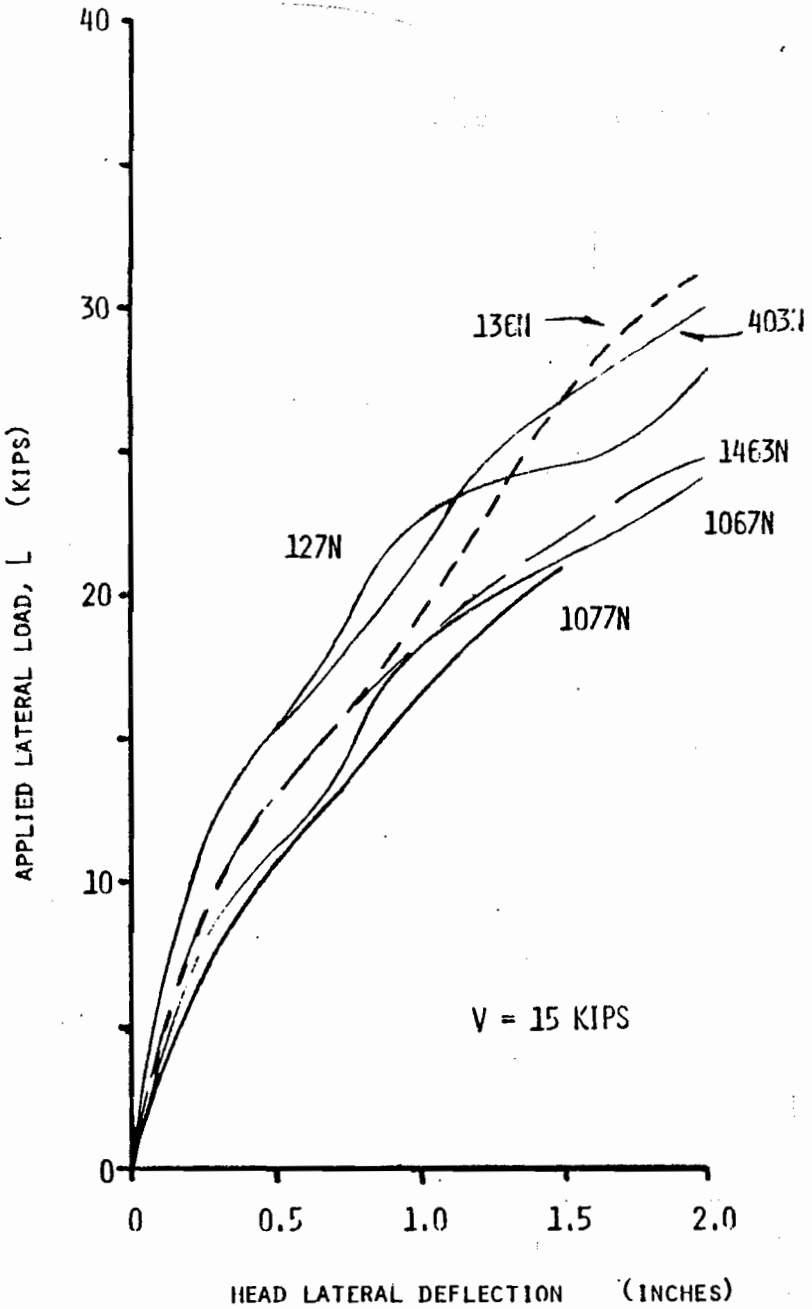

TIE DESCRIPTION

127:	DEGRADED TIE; ADJACENT TIE DEGRADED; TIE #126 MOVED AGAINGT TIE #125
136:	WORN NONDEFECTIVE TIE; ADJACENT TIES NONDEFECTIVE; AFTER 1st CYCLE WITH V=5 KIPS
403:	DEGRADED TIE; ADJACENT TIES DEGRADED
1067:	TIE #1066, #1067, AND #1068 REMOVED
1077:	TIE #1077 AND #1078 REMOVED
1463:	GOOD TIE; JOINT BOLTS REMOVED

FIG. 4.2 - LOWER BOUND FIELD TEST SUMMARY

field test values of the highest or lowest lateral load in any test for a given displacement. For example, the 15 kips vertical load composite for the lower bound was found by averaging lateral load levels at constant deflections of 0.5, 1.0, and 2.0 inches for the two tie conditions previously mentioned. These two cases where chosen to be averaged since these cases yield the lowest lateral load at these deflections (see Figure 4.3). Similarly, other upper and lower bound composites were found.

The parametric identification was performed to find the component resistance characteristics that when used with the analytical model would reasonably predict the upper and lower bound test results. Figure 4.3 shows the results of the parameter search as component characteristics for varying degrees of stiffness, i.e., upper and lower bounds. These bounds, however, are representative only of low speed tracks. Using the parameter values shown in Figure 4.3 extreme responses were predicted using the analytical model. The results of these predictions are compared to the field test composite curves in Figure 4.4 for varying vertical loads. For the V = 15 kip case, at 1 inch deflection the predicted and field test composite curves differ by approximately 5 percent for both rail head and rail base deflections. Although the 30 kips vertical case is not as closely coincident as the 15 kips case, the basic agreement is quite remarkable.

The difference in agreement for varying vertical loads may imply that the field test composite behavior does not project readily to other vertical load results. That is, a given type of support configuration can be related through the effect on the vertical and lateral component resistance. However, the composite may not appear in the sampling at other vertical loads. The consequences of this behavior is shown in lateral-vertical load constant deflection plots. As shown in Figure 4.5 lines of constant displacement for lateral load are nearly linear functions of vertical load in the model predictions when the parameters are fixed. From field test data, however, the composite curve can be controlled by different stiffness values over the complete range of test displacements. Note that the model predictions yield slightly stiffer responses than the field test composites except at the values where the vertical load is 30 kips. It appears that the system and component responses are smeared by the test configurations. That is, the beam load

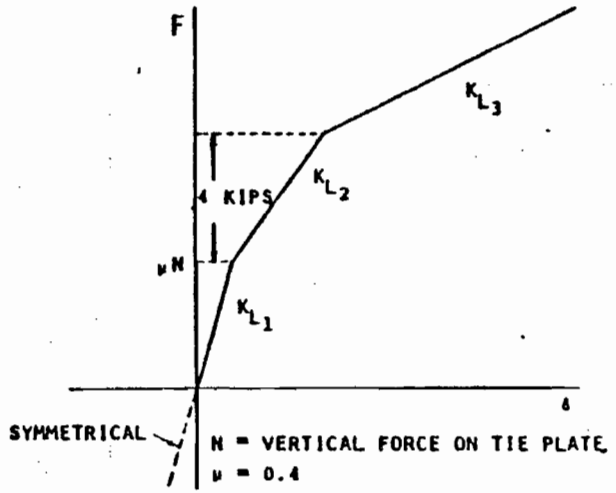

NONLINEAR LATERAL SPRING

	LOWER BOUND	AVERAGE	UPPER BOUND
K_{L1}	40 K/IN	60 K/IN	80 K/IN
K_{L2}	6 K/IN	12 K/IN	18 K/IN
K_{L3}	0.8 K/IN	3 K/IN	5 K/IN

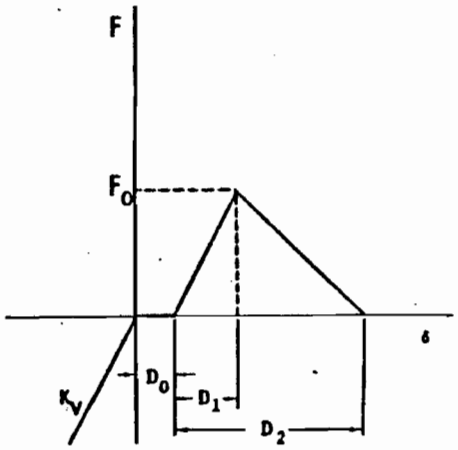

F_0 = PEAK SPIKE PULL OUT FORCE

D_0 = GAP BETWEEN SPIKE HEAD AND UPPER RAIL BASE SURFACE

NONLINEAR VERTICAL SPRING

	LOWER BOUND	AVERAGE	UPPER BOUND
F_0	2 KIPS	3 KIPS	4 KIPS
D_0	0 IN.	0 IN.	0.2 IN.
D_1	0.2 IN.	0.2 IN.	0.2 IN.
D_2	1.5 IN.	1.5 IN.	1.5 IN.
K	25 K/IN.	40 K/IN.	60 K/IN.

FIG. 4.3 - COMPONENT CHARACTERISTICS

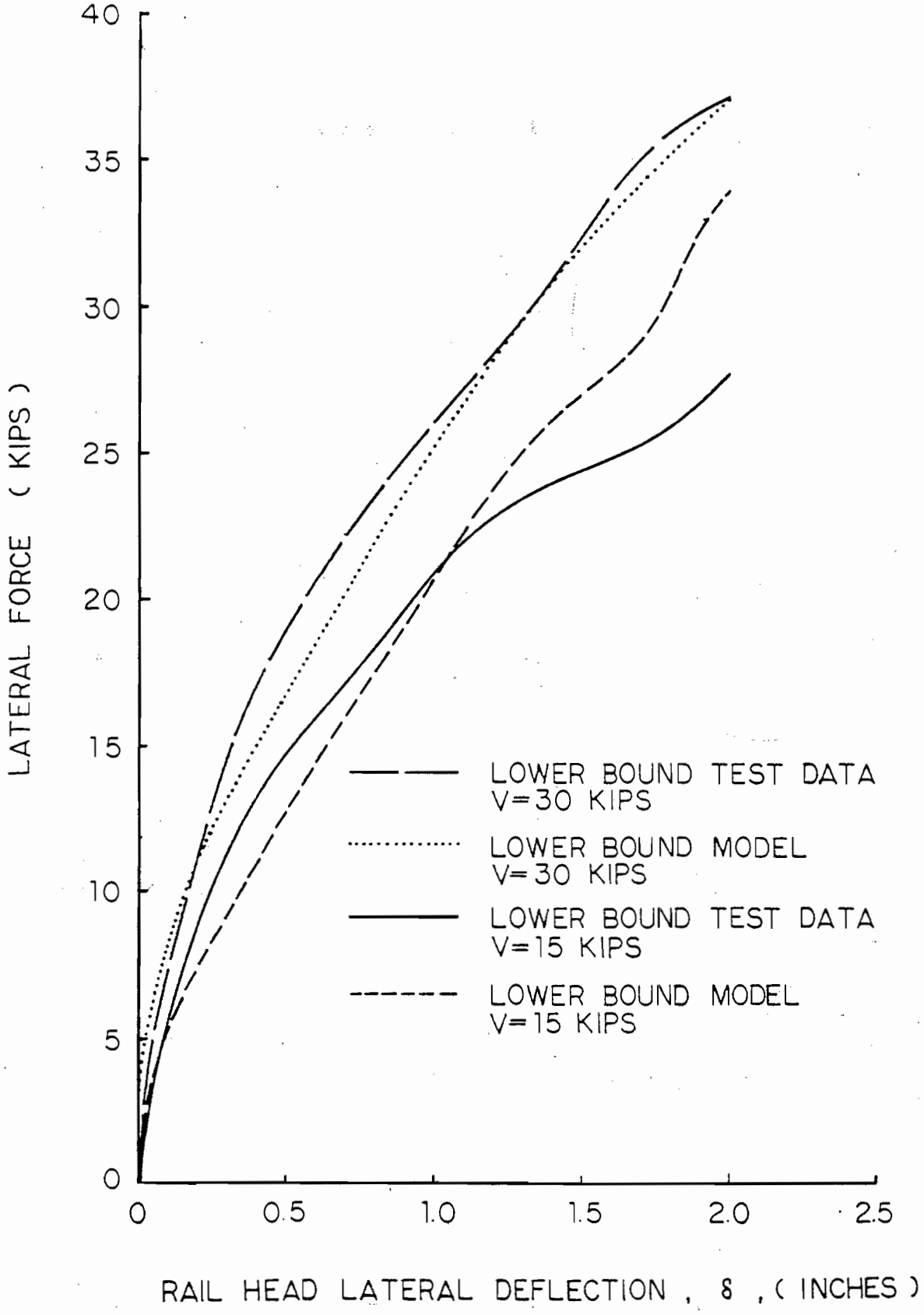

FIG. 4.4 - ANALYTICAL VERSUS EXPERIMENTAL LOAD-DEFLECTION BEHAVIOR

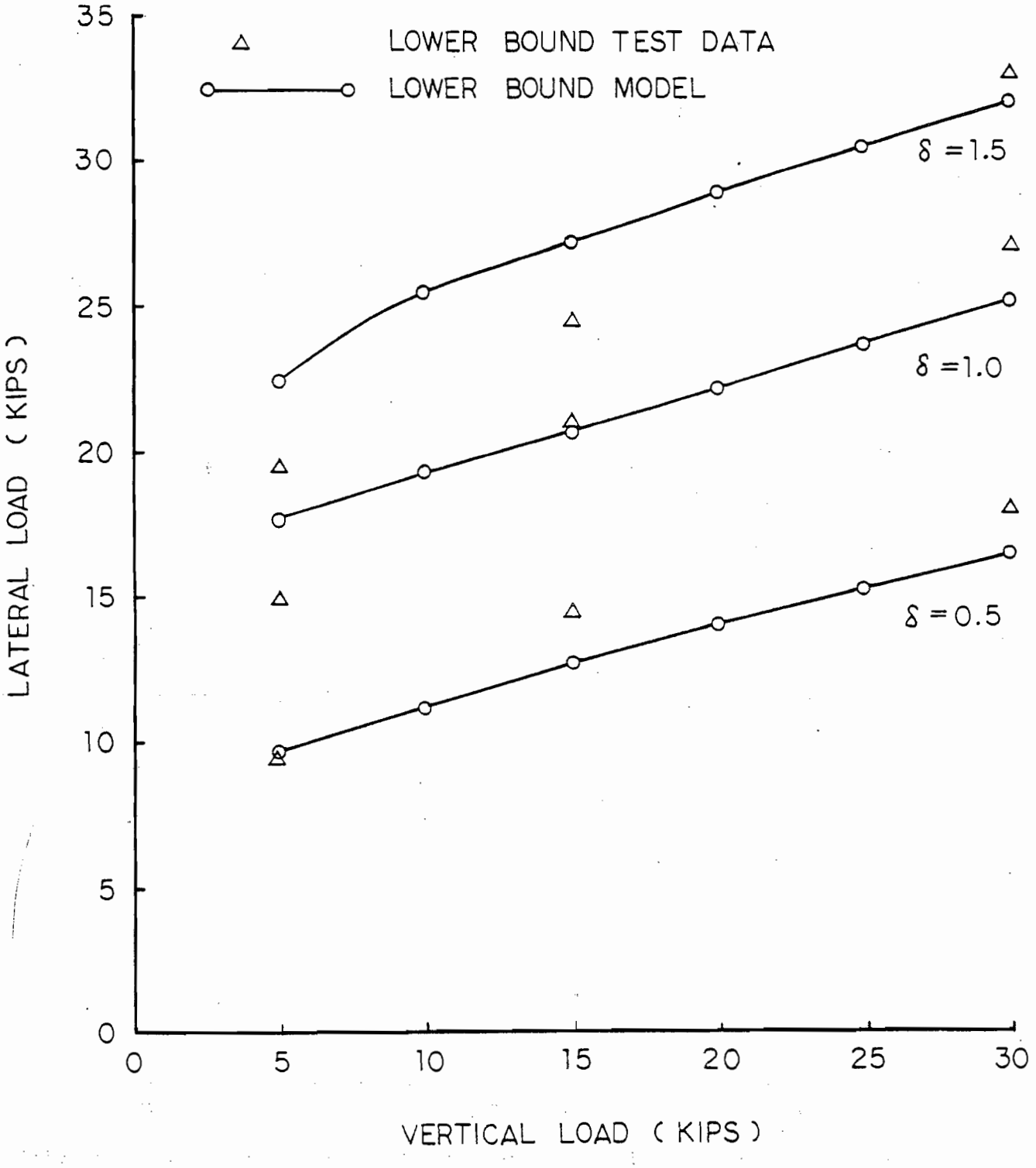

FIG. 4.5 - LATERAL LOAD VERSUS VERTICAL LOAD CURVE (LOWER BOUND)

transfer as well as support stiffness variation tie to tie for each vertical load contribute to project the composite pattern shown in the lines of constant displacement. Figure 4.6 shows the average field test data compared to the predicted average support but with the loaded tie simulated by lower bound support. Note that the lines of constant deflection are nearly linear for each case.

4.2 Single Versus Multiple Loads

In order to relate the track responses defined in the field tests conducted with a single set of spreading loads to the strength required by vehicle loading, truck load conditions must be taken into consideration.

The principle of linear superposition and the theorem of reciprocity were utilized as a means to investigate the effect of multiple loads. Figure 4.7 compares the results of the linear superposition to the multiple load responses from the model predictions. It can be seen that up to the 25 kip lateral load level that linear superposition is quite accurate when compared to the multiple load prediction. Beyond this point, however, the curves are distinctly different.

Figure 4.8 illustrates the variation in vertical load for multiple loads. Again, the presence of vertical load strengthening the resistance against gauge widening can be seen. The vertical and lateral loads are identical for each axle in this case.

As indicated by Figure 4.9 a given total truck load is more severe when all of it is applied at one axle than when the same load is divided between two axles. However, from Figure 4.10, the worst case truck loading for a given vehicle can easily be a combination of axle loads when compared with the maximum found at any single axle.

4.3 Influence of Track Variations

Using the component resistance characteristics found through the identification process, the analytical model was used to predict the effect of variations in certain track parameters. Specifically, the effects of rail weight, missing ties, broken rail, and joint bars on lateral load capacity are examined.

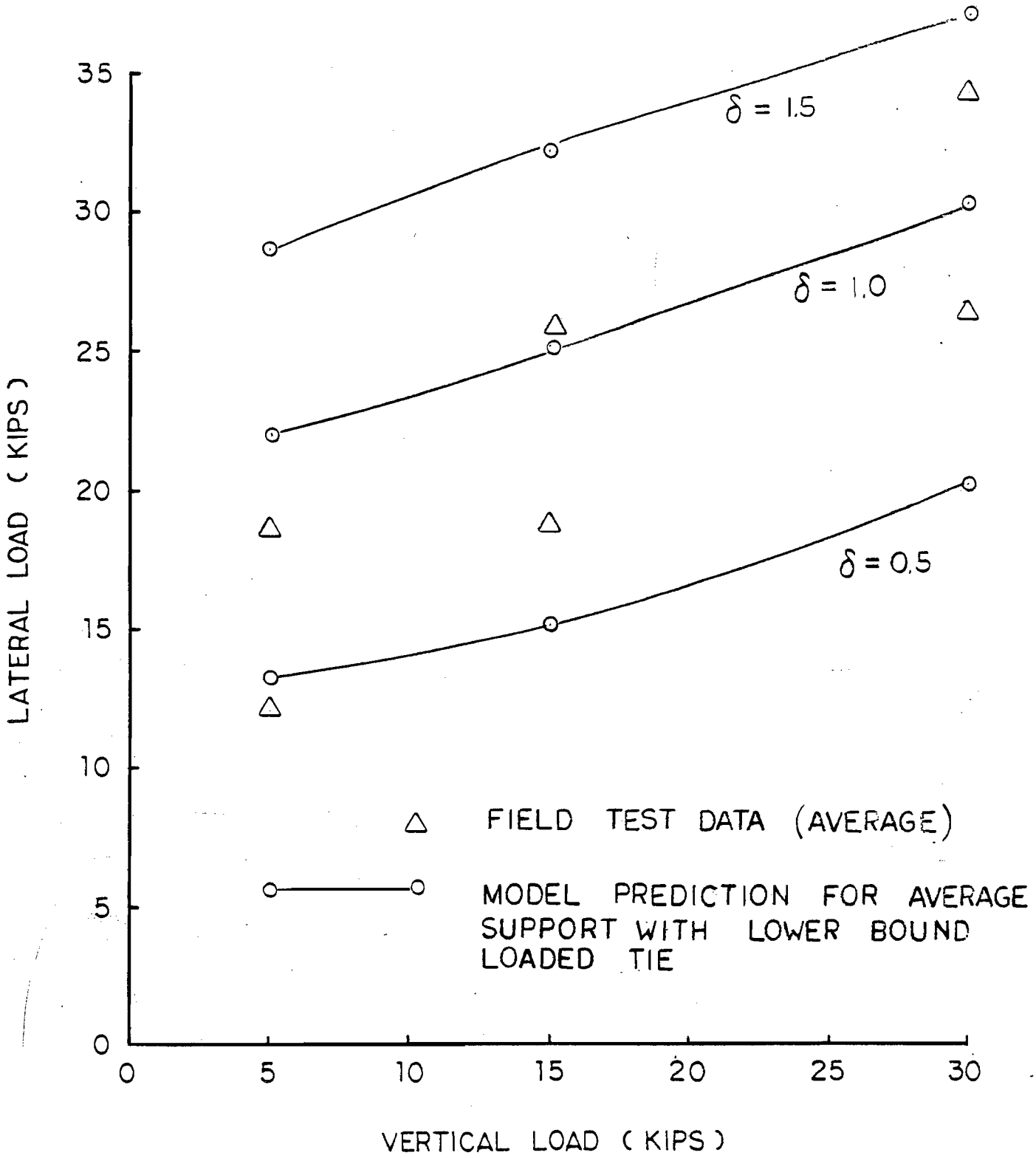

FIG. 4.6 – LATERAL LOAD VERSUS VERTICAL LOAD CURVE (AVERAGE OF DATA)

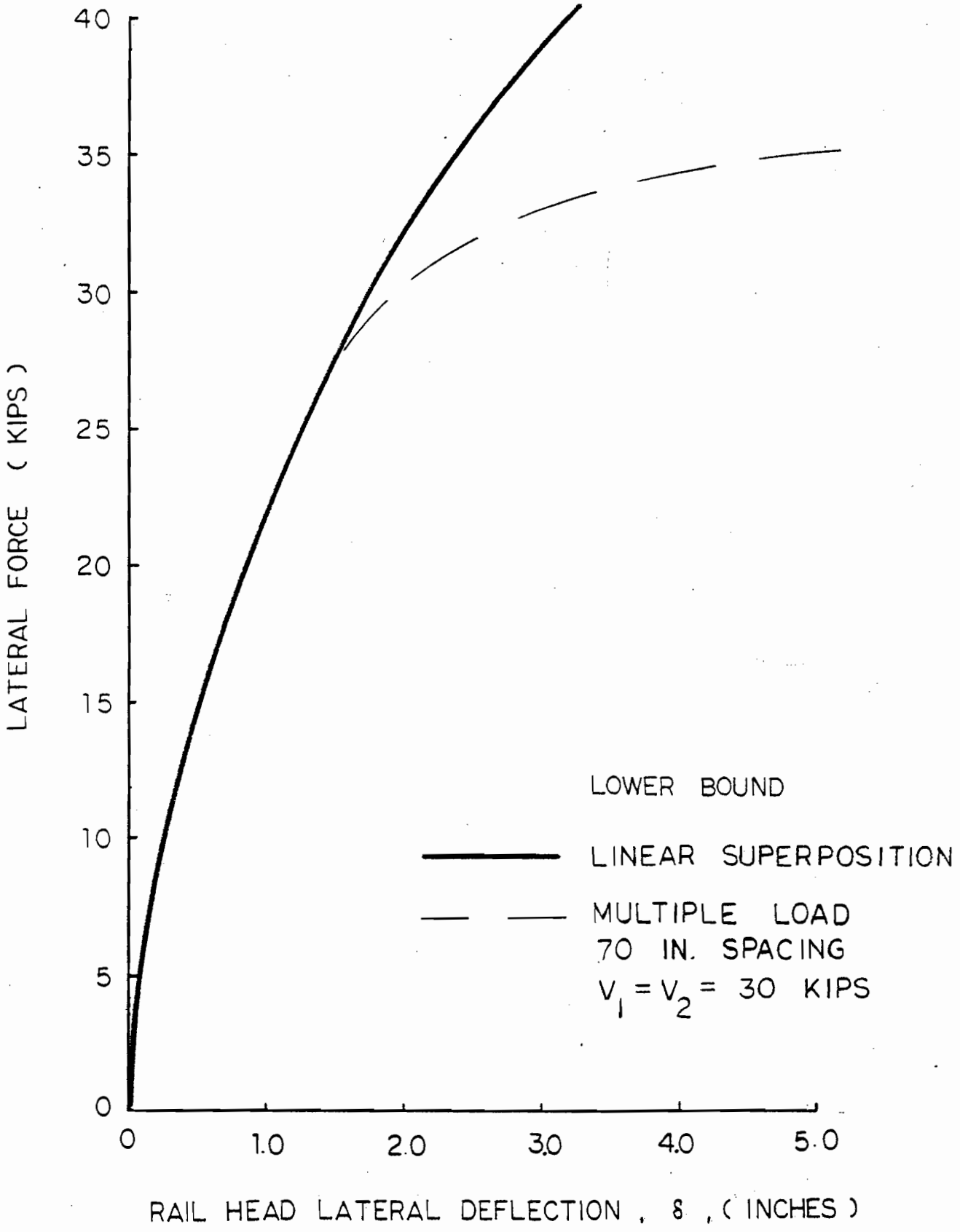

FIG. 4.7 - COMPARISON OF LINEAR SUPERPOSITION TO ACTUAL MULTIPLE LOADING CASE

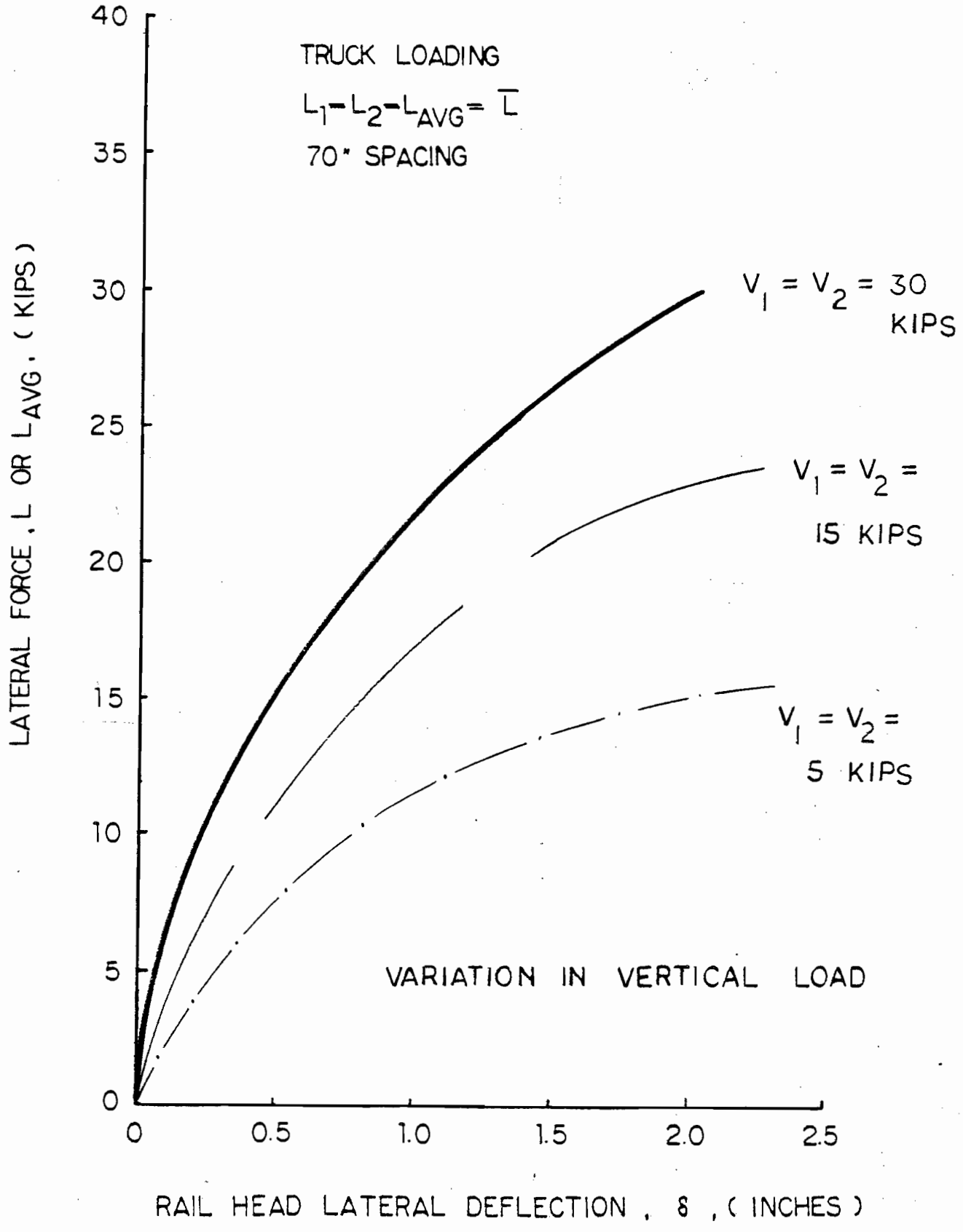

FIG 4.8 - VARIATION OF VERTICAL LOAD FOR MULTIPLE LOADING

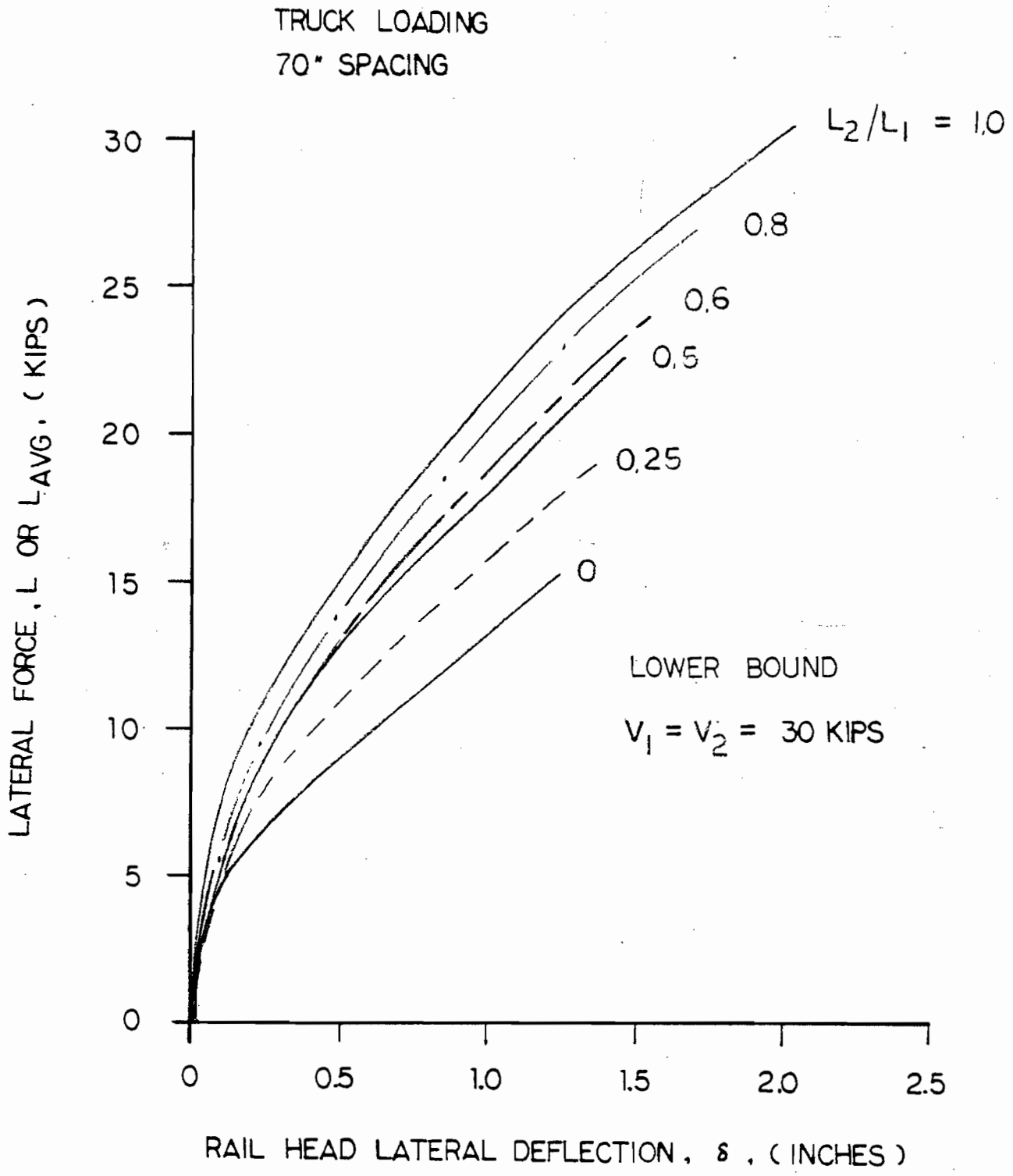

FIG. 4.9 - VARIATION OF TRAILING AXLE LOAD FOR MULTIPLE LOADING

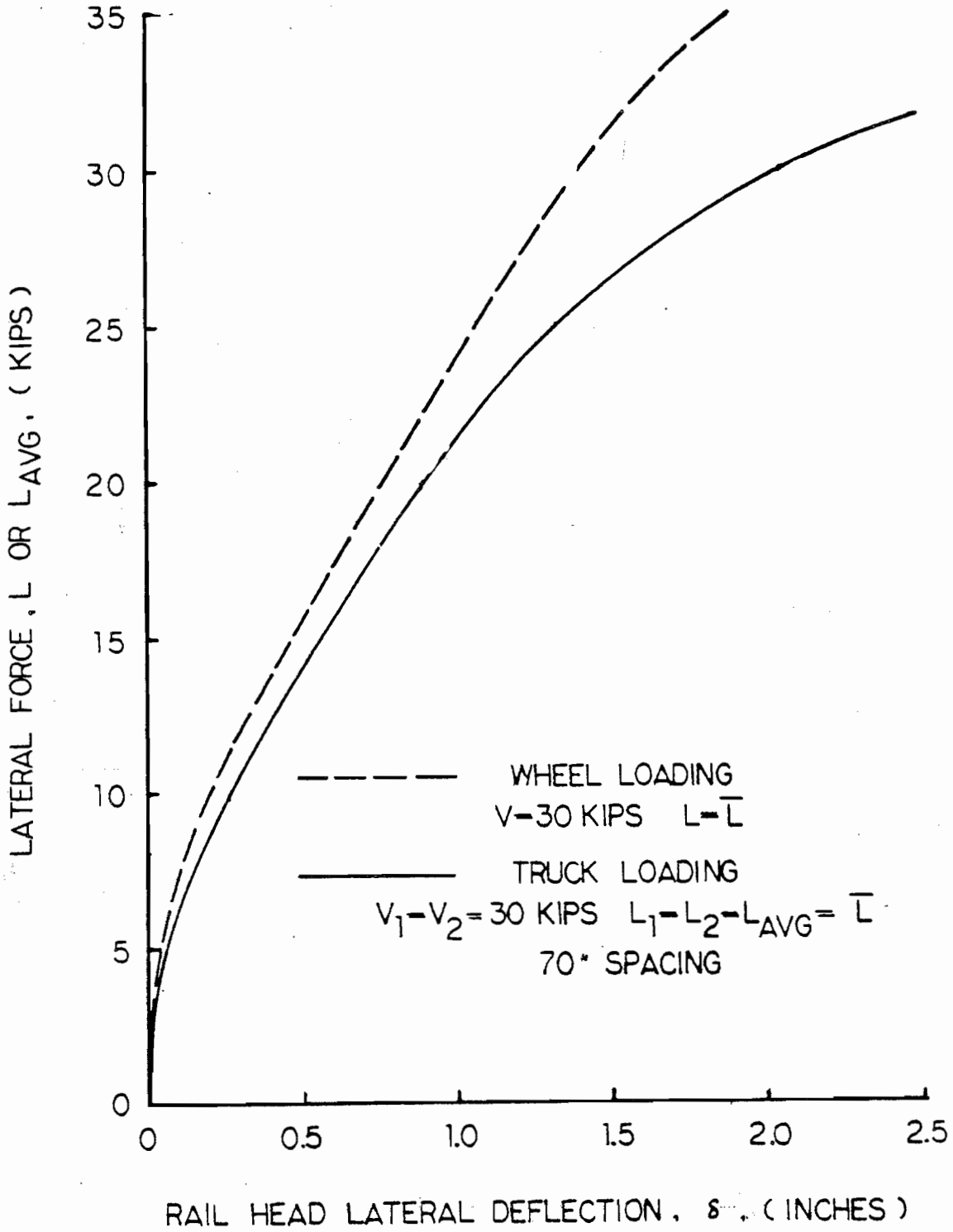

FIG. 4.10 - COMPARISON OF WHEEL LOADING TO TRUCK LOADING

4.3.1 Rail Weight

Figure 4.11 indicates the influence of rail weight on the predicted response. In the initial roughly linear region of the response curve, the geometry of the rail cross section seems to control the effect. In particular, the width of the rail head and the distance from the gauge corner to the shear center are the critical dimensions. Recall from Section 2.0 that these two dimensions define the value of the moment causing the twisting of the rail. In this nearly linear regime, however, the differences in response are relatively small for all rails. At higher lateral loads the response of light rail softens more than heavier rail sections as stiffness properties begin to dominate over the geometric effects.

4.3.2 Missing Ties

The effect of degraded or expectedly weak track on the response characteristics of load versus deflection is investigated. Figures 4.12 shows the results of using the lower bound stiffness characteristics for a variety of missing tie conditions.

Figure 4.13 shows extreme cases for upper and lower bound stiffnesses and for zero and three missing ties. These results show that the upper bound model for the three missing tie case gives less lateral support than the lower bound model with no missing ties. Therefore, the significance of this plot is that for the conditions considered higher stiffness parameters cannot adequately compensate for the lack of support.

4.3.3 Joint Bars

The effect of missing joint bars or of broken rail on lateral strength of rail is now examined. Recall in the analytical model that the rail is modeled as a beam with fixed ends while the support of the ties is represented by nonlinear springs. In order to investigate the effect of missing joint bars and broken rail the model was altered where only one end of the rail is fixed and the other rail left free.

Figure 4.14 shows the rail head and rail base characteristics of a rail with a missing joint bar or a broken rail. Note that only one set of loads is

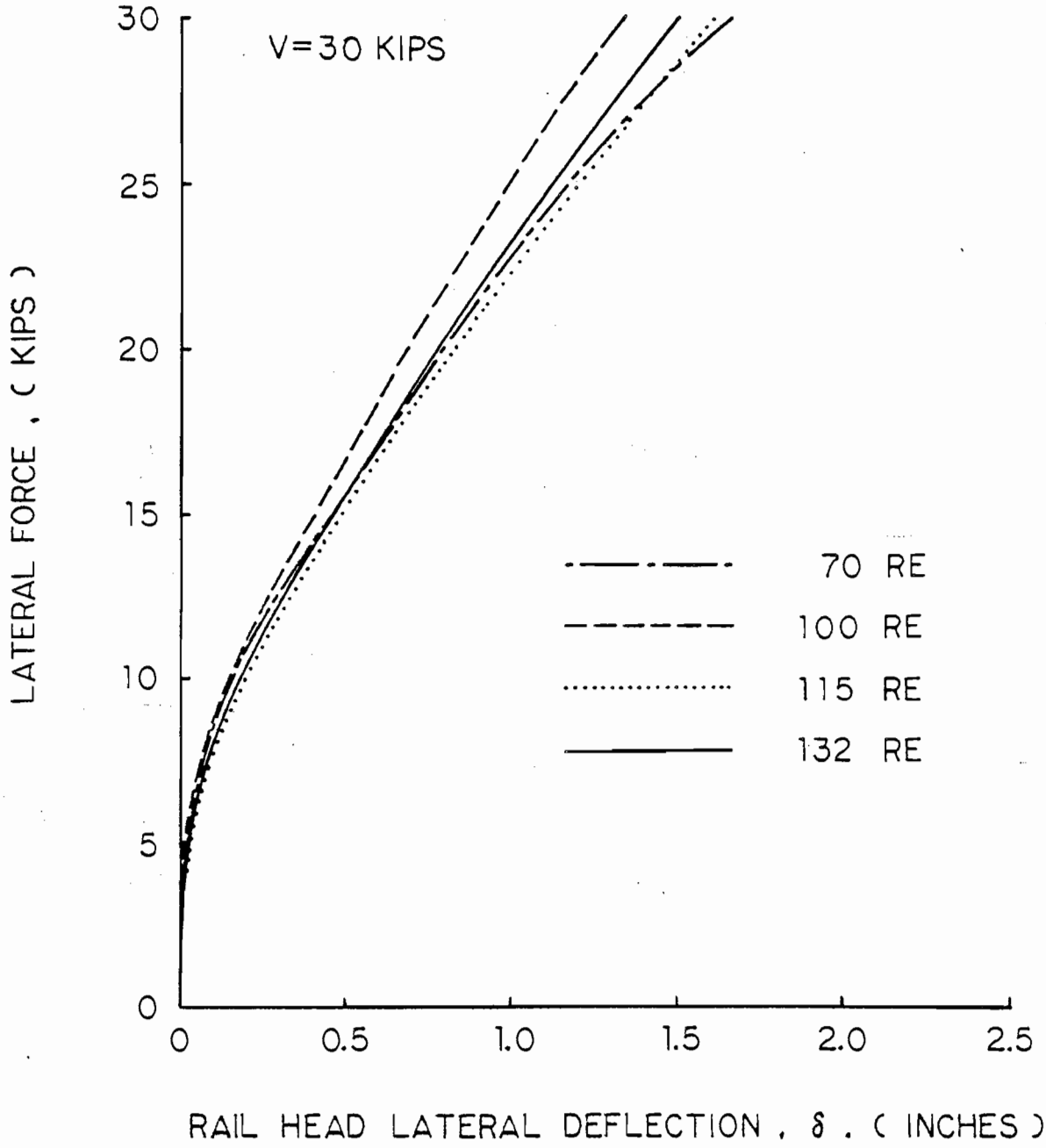

FIG. 4.11 - EFFECT OF RAIL SIZE ON LOAD-DEFLECTION BEHAVIOR

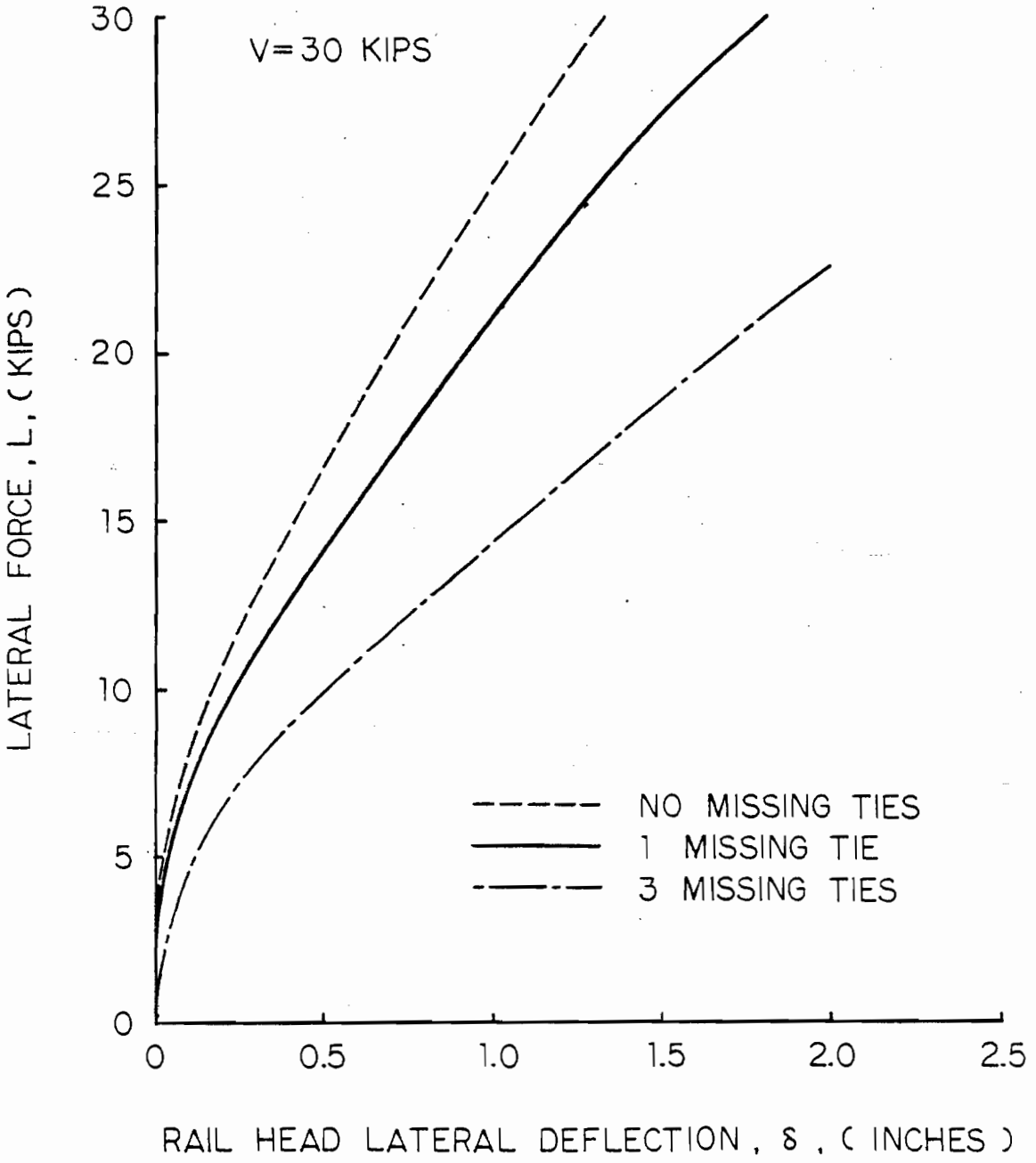

FIG. 4.12 - VARYING MISSING TIE CASE

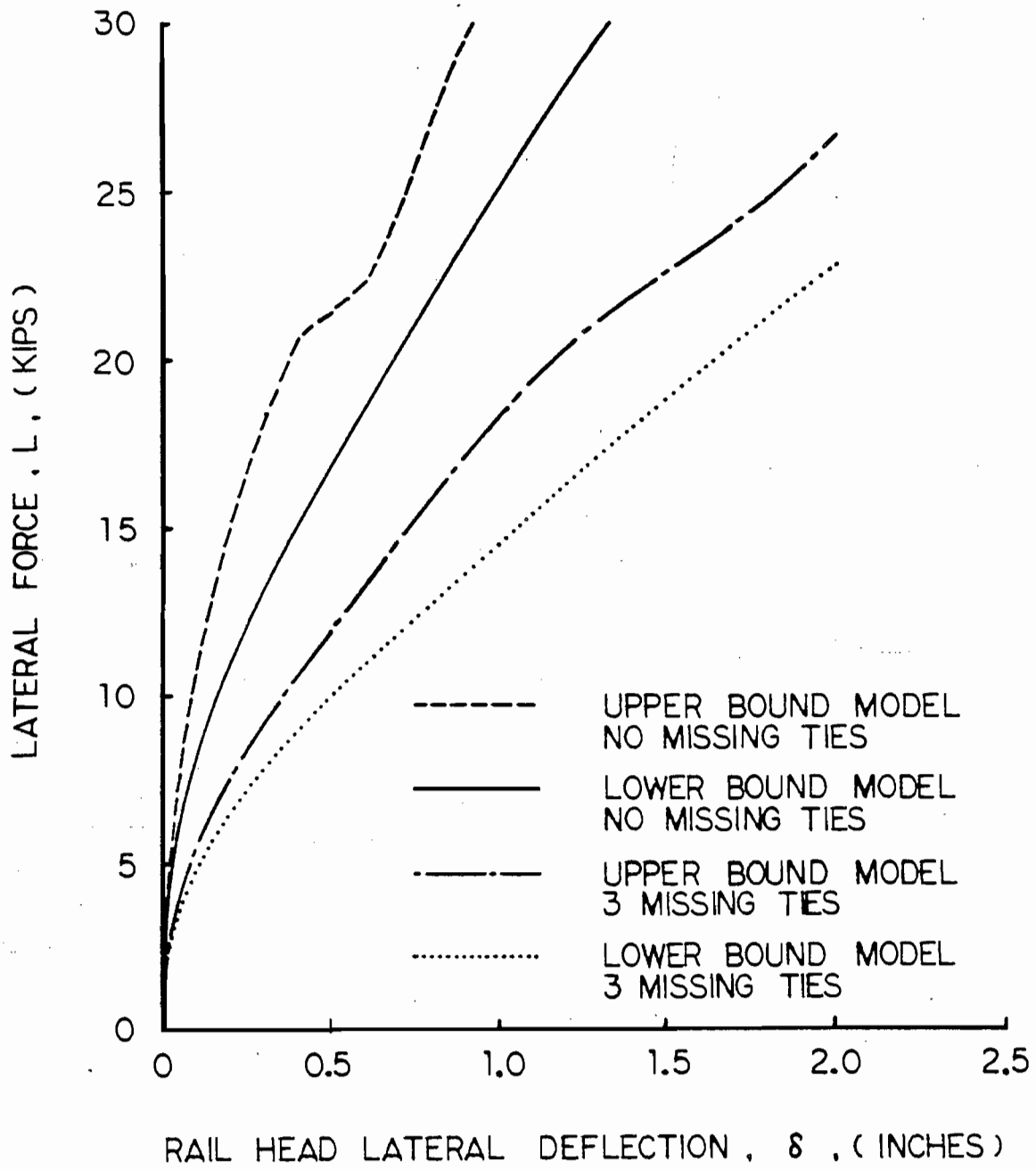

FIG. 4.13 - EXTREME MISSING TIE CASES

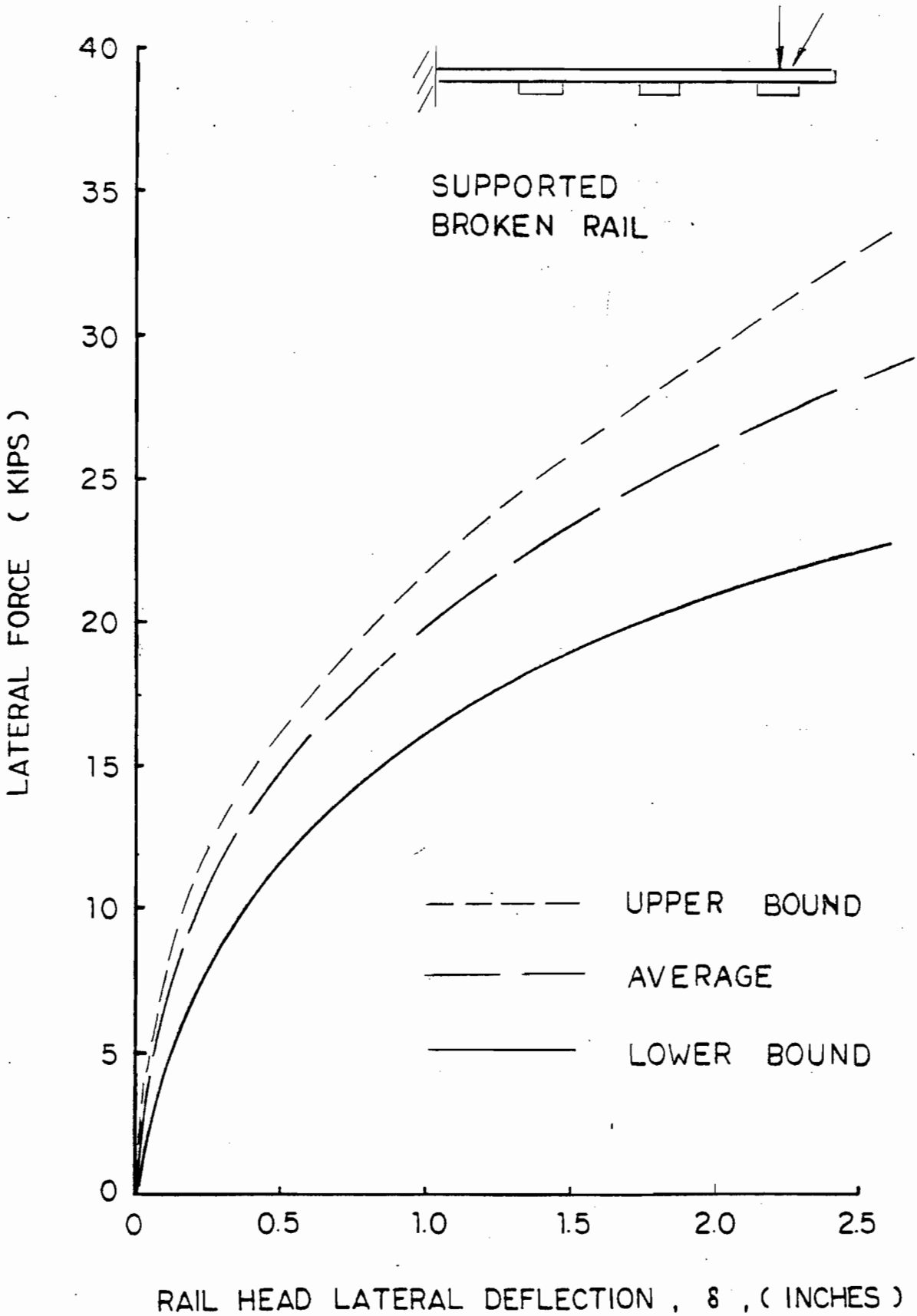

FIG. 4.14 - VARIATION OF STIFFNESS PARAMETERS FOR BROKEN RAIL OR MISSING JOINT BAR (SUPPORTED)

applied and a vertical load of 30 kips is used. This plot shows that for this rail configuration that the difference in lateral strength at a rail head displacement of 1 inch is about 17 percent between average and lower bound support. The same rail configuration is modeled for truck loading, i.e., a pair of loads and the result is shown in Figure 4.15 for the rail head response. A decrease in capacity (lateral strength) for the truck loading versus the single load is evidenced. The reduction in lateral strength from average to lower bound stiffness, however, is on the same order (about 18%) at the 1 inch rail head deflection for the multiple loading as for the single load. Further examination of the variation in stiffness characteristics is displayed in Figure 4.16. An added irregularity of this result is that the free end yields no support. As can be seen, the curves for average and lower bound stiffness are quite flat.

4.3.4 Spike Gap

In the selection of the vertical component stiffness, a loss mechanism was described where the distance between the rail base and the spike head would yield no resistance if the spike had been pulled out to such a distance previously. In this section a gap of 0.2 inches was incorporated into the stiffness parameters and the effects of this spike gap were examined. Figure 4.17 shows the difference in employing the loss mechanism on the response curves for lower bound and average support. As can be seen the presence of the gap decreases the lateral strength on the order of 5 percent at one (1) inch of rail head deflection for both support characteristics. Figure 4.18 shows similar information, but also shows the upper bound support. An interesting subfeature of these results is the distinction between the monotonically softening response for low stiffness parameters (as shown in the sections describing missing ties and joint bars) in contrast with the "S" response of the upper bound springs shown here. In this case the upper bound behavior is directly related to the spike head to rail base gap. This distinction, however, is clearly apparent in the typical test results for worn ties at the Logan field test (softening) and the "S" behavior characteristic of the AAR Laboratory tests [2] using new ties with substantial gaps induced by cyclic loading of the track.

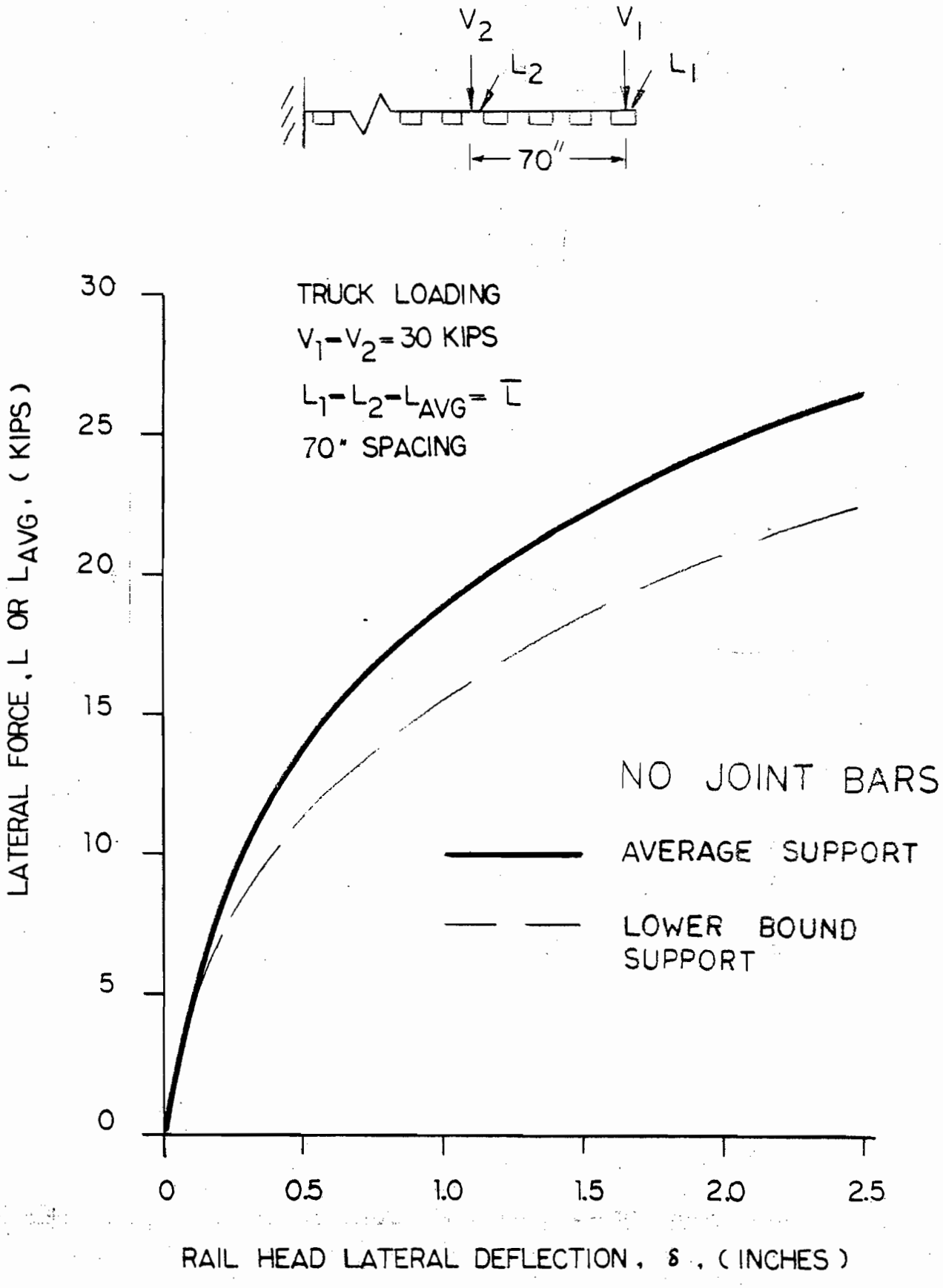

FIG. 4.15 - VARIATION OF STIFFNESS PARAMETERS FOR BROKEN RAIL OR MISSING JOINT BAR (UNSUPPORTED)

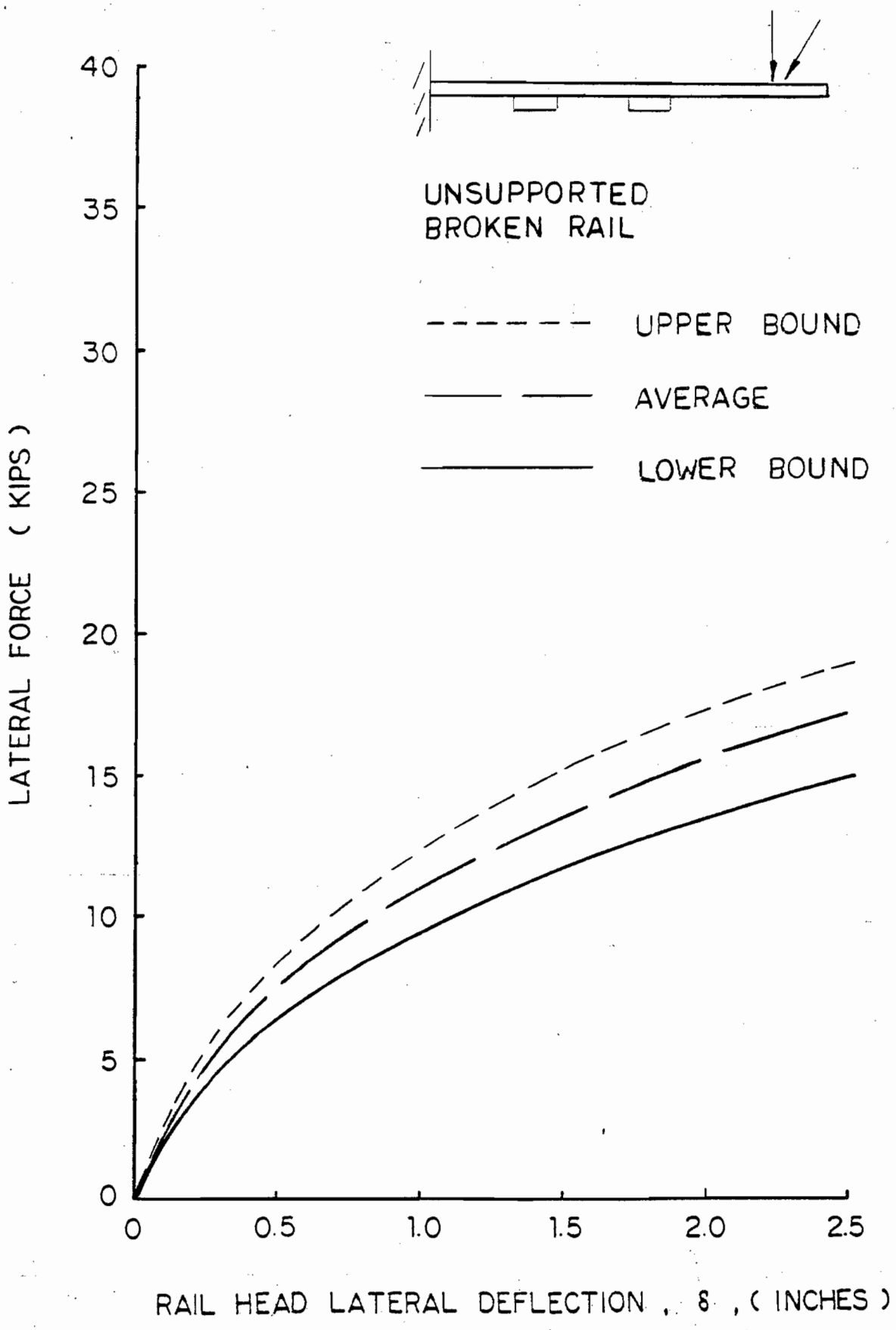

FIG. 4.16 - TRUCK LOADING FOR MISSING JOINT BAR CASE

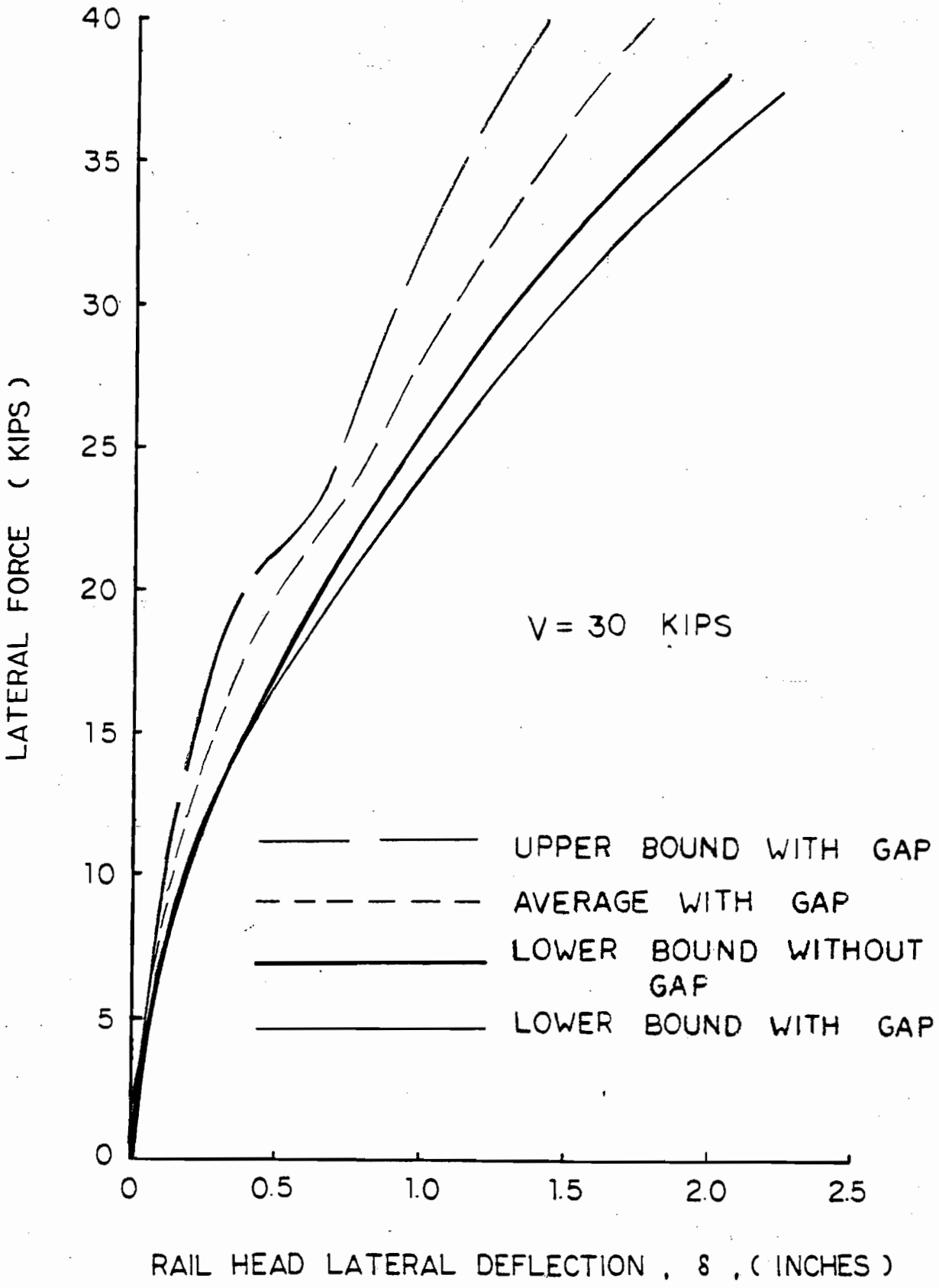

FIG. 4.17 - EFFECT OF SPIKE GAP ON VARYING STIFFNESS PARAMETERS (WHEEL LOADING)

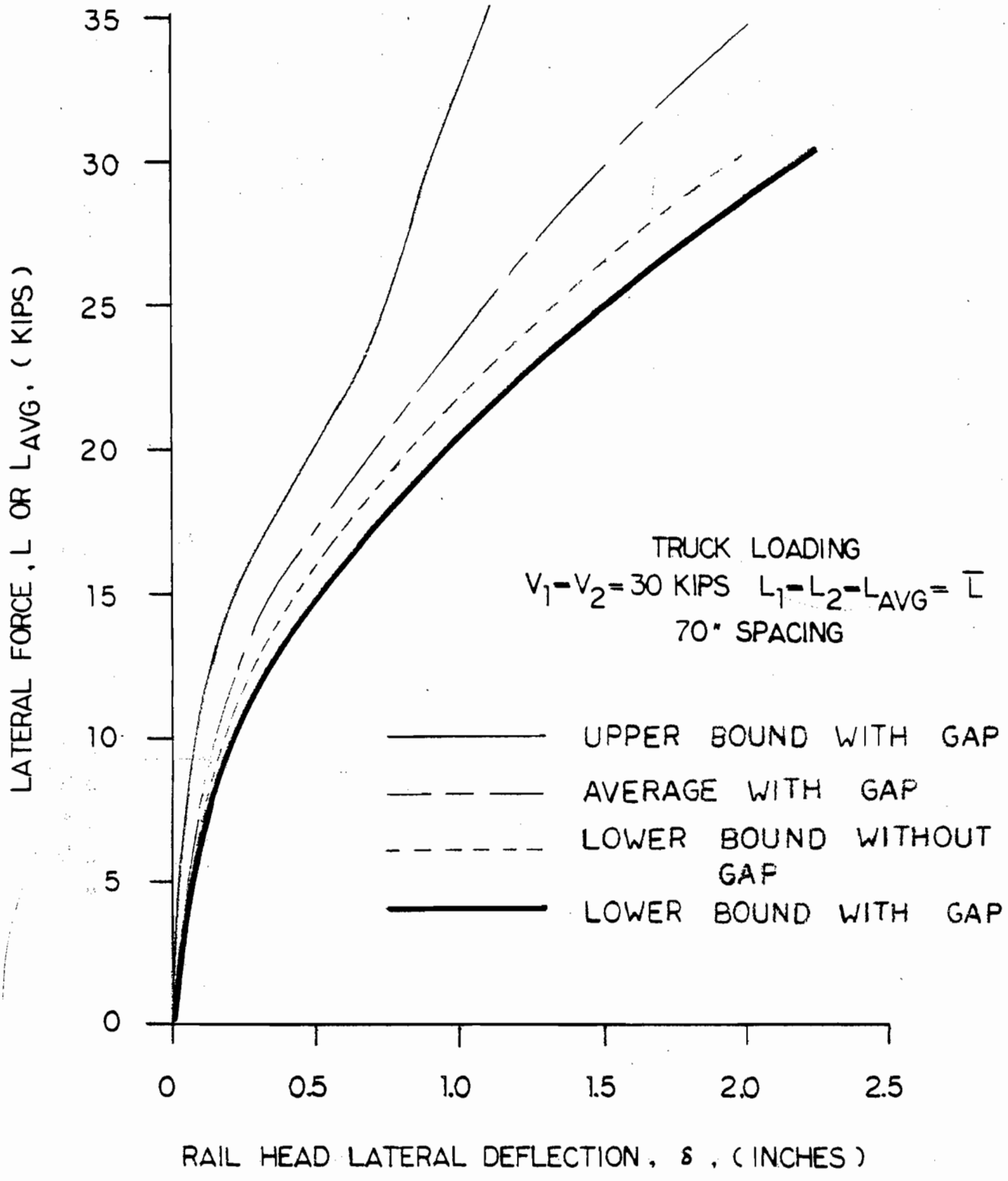

FIG. 4.18 - EFFECT OF SPIKE GAP ON VARYING STIFFNESS PARAMETERS (TRUCK LOADING)

5. CONCLUSIONS

The analysis described in Section 4. can be summarized as follows:

a) The Logan field test data were reduced to obtain lower bounds on lateral strength capacity and component characteristics

b) The analytical model was used along with the appropriate component characteristics to extrapolate track variations which include:

   i. influence of multiple (truck) loads
   ii. different rail weights
   iii. a range of support conditions.

The results of this analysis have identified the key parameters that describe the strength and failure mechanism. Other results of the parametric studies may be highlighted as follows:

a) Truck, rather than single-axle loads, represented the most severe demand on the track, causing the largest gauge spreading deformation.

b) The lateral load versus rail head deflection response is not strongly influenced by rail size variation due to the fixed height-to-strength characteristics of the rails.

Further extrapolation of the field test data using the analytical model may be performed to determine the minimum required strength of track in terms of rail head deflection under load. That is, a minimum performance requirement for rail restraint based on lower bound condition can be developed which would be of important use in the prevention of derailments due to gauge spreading-rail overturn on track in service for speeds up to 25 MPH.

6. APPLICATIONS AND RECOMMENDATIONS FOR FURTHER WORK

The results of the parametric studies described in Section 4. were presented in the form of lateral load versus rail head deflection curves. Having developed an analytical model to predict load-deflection responses of rail as well as having identified the key parameters describing rail strength and the failure mechanism, the means for determining the capacity of low speed track necessary to provide adequate lateral restraint to prevent gauge widening failure are now available. A single load-deflection curve can be formulated to characterize the track capacity for all admissible track geometries. This load-deflection curve can then be used as a specification curve which would be intended to reduce the incidence of wide gauge or rail spreading derailments. Furthermore, the same procedure can also be used to extrapolate results to cases of track support to higher speed track. The basis for developing such a specification is the establishment of the minimum strength against shifting or overturning of the rail under train loads. An approach in quantifying the specification may be outlined as follows:

- Define the strength of minimally adequate track
- Define peak loads
- Evaluate Margin of Safety
- Define specification and compliance approach

In evaluating the margin of safety, consider that the application of lateral spreading loads, L_l and L_r cause rail deflections δ_r and δ_l which increase the distance between the rails or the gauge, g. The amount that thee rails displace is dependent on the vertical load and the lateral restraint of the rails. If the lateral support is not sufficient, the total outward deflection, $\delta_l + \delta_r$, can exceed the available tread width or distance to drop, D, that would remain on deformed rails [18].

In practice, the condition where the total deflection plus the gauge distance is greater than or equal to 59-1/2 ", or $g + \delta_l + \delta_r > 59\text{-}1/2"$, is considered to be unsafe. A safety criterion for rail restraint capacity can now be defined as:

$$D \geq \delta_l + \delta_r$$

These concepts are shown schematically in Figure 6.1.

Since rail geometry and stiffness vary along the track, the distance to drop, D, and the rail deflections δ_l and δ_r resulting from wheel-rail interaction are functions of their location. Critical sites for rail restraint capacity can be identified by the condition:

$$D - (\delta_l + \delta_r) = \text{minimum}$$

A location satisfying this equation generally occurs in the vicinity of minimum D and maximum lateral truck load. Since spreading loads are of comparable magnitude, it is convenient to consider a single rail and adopt a conservative criterion, namely,

$$\overline{D}_{allow} - \delta_{max} > 0$$

where δ_{max} is the larger deflection between δ_l and δ_r and the subscripts refer to maximum values along the track. The term D_{allow} is the critical, allowable rail head deflection and will be used to define the requirement for minimum rail restraint.

Careful consideration must also be given to vehicle track interaction. That is, a distinction between track deflections and the lateral movement of the axle must be made. Lateral axle loads depend on the type, amplitude, and combination of gage and alinement variations encountered on track. Since the wheel-rail contact point as well as the rails can move laterally, some loading conditions can be ignored in terms of restraint capacity. These conditions would lead to wheel lift or wide gauge failure even on absolutely rigid track. The deviations that cause such response are designated as geometrically inadmissible.

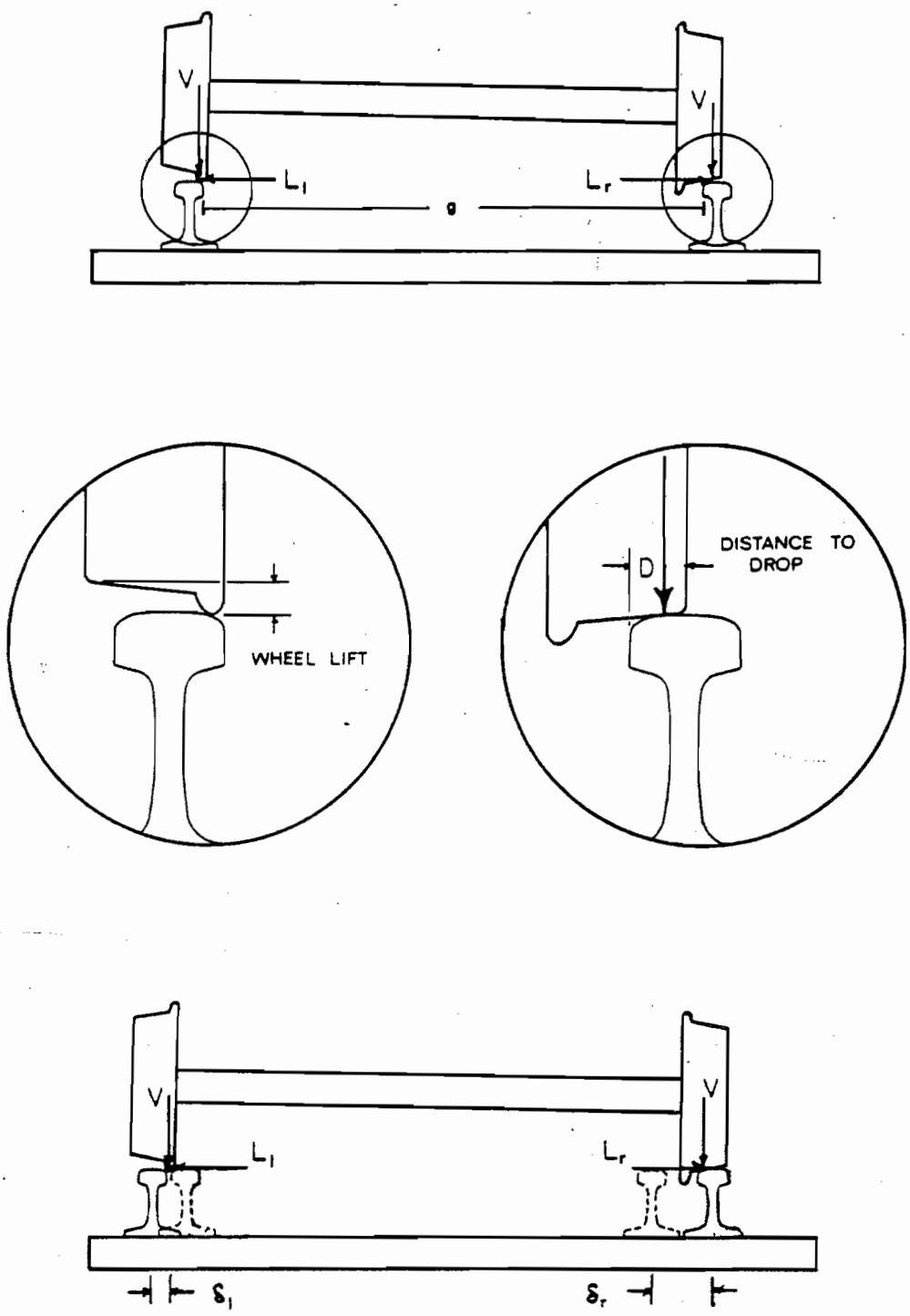

FIG. 6.1 - SCHEMATIC OF MARGIN OF SAFETY CONCEPT

Figure 6.2 is a schematic definition of restraint capacity. Each point represents a maximum load and corresponding D_{allow} of a track with a given type of admissible variation in track geometry. It would be too conservative to define minimum requirements for rail restraint on the basis of maximum loads expected anywhere on the track and the minimum allowable total head movement of the entire track. Safe operation is assured if the minimum strength (L versus δ) curve lies above all the points of the admissible geometry and load.

For low speed North American track, 100-ton hopper cars are vehicles considered to define the worst conditions. On curved track, it is their truck loads that are critical values. Figure 6.3 shows data pairing maximum lateral load and distance to drop for the types, amplitudes, and combinations of gauge and alinement variations used to represent the track geometry. The region beyond the dotted line boundary denotes geometrically inadmissible conditions, wheel lift greater than 0.6 inches or maximum static gauge greater than 59.0 inches.

The remaining admissible maximum load conditions can then be compared with the curve describing the maximum measured capacity of the track. By superimposing a load-deflection curve which defines the minimum required strength onto curves such as Figure 6.3, geometry and load conditions likely to cause failure by gauge spreading can be found.

The specification developed in this study provides that all crosstie and spiking conditions are acceptable except in cases where the load capacity of a location on track falls below the required minimum. Load capacity is determined by a controlled load versus deflection test of the rails at a suspect location. For track with adequate capacity the test may be suspended at small deflections if the test load exceeds the passing load limit, as shown in Figure 6.4. Suspect locations are initially to be identified by visual examination. A stationary (static) test is then performed using a device such as the Track Loading Fixture (TLF). The lateral rail head displacement is monitored with the level of lateral load. Finally, the test loads are compared at the displacements referred to in Figure 6.4 for pass-fail criteria.

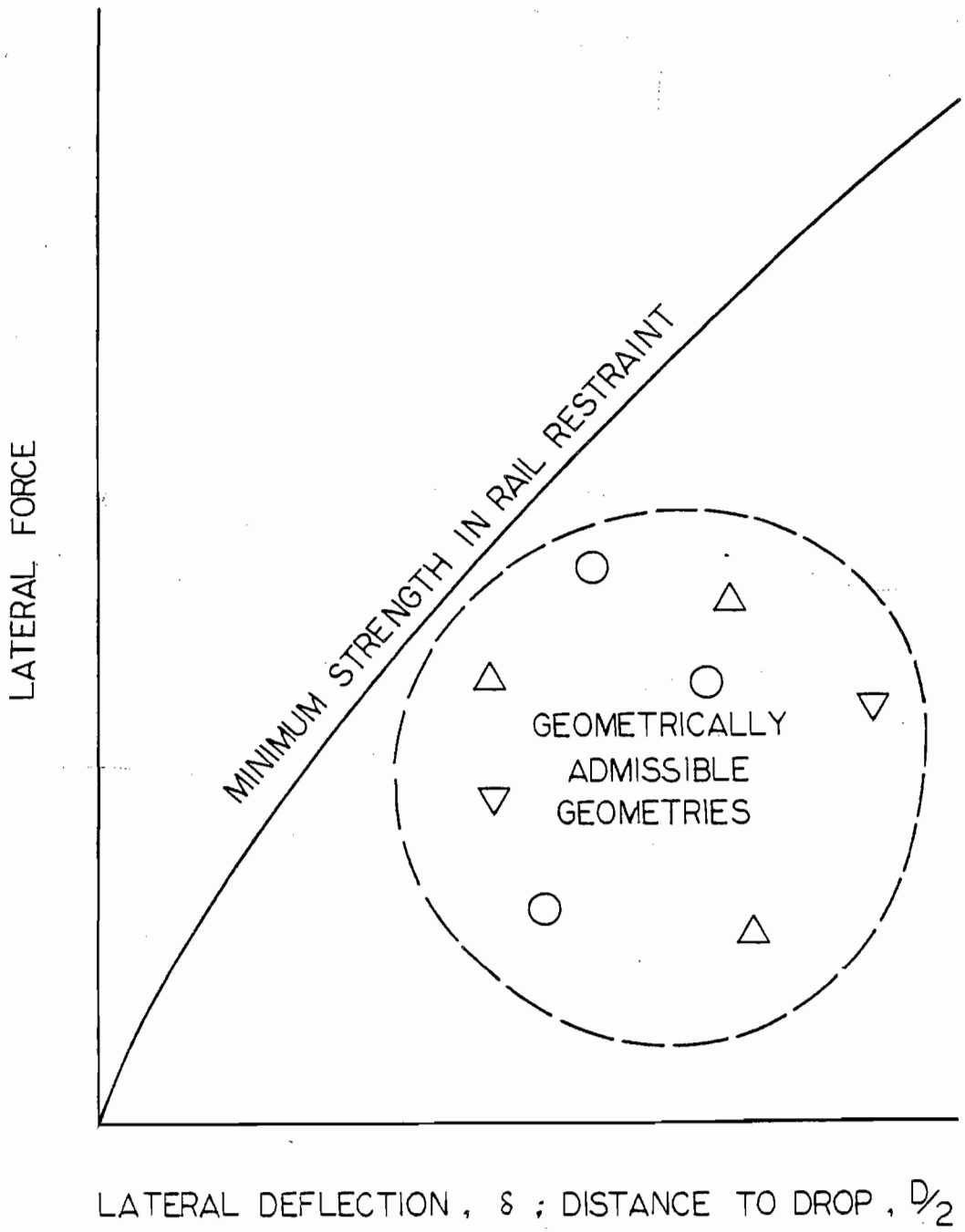

FIG. 6.2 - SCHEMATIC DEFINITION OF RAIL RESTRAINT CAPACITY

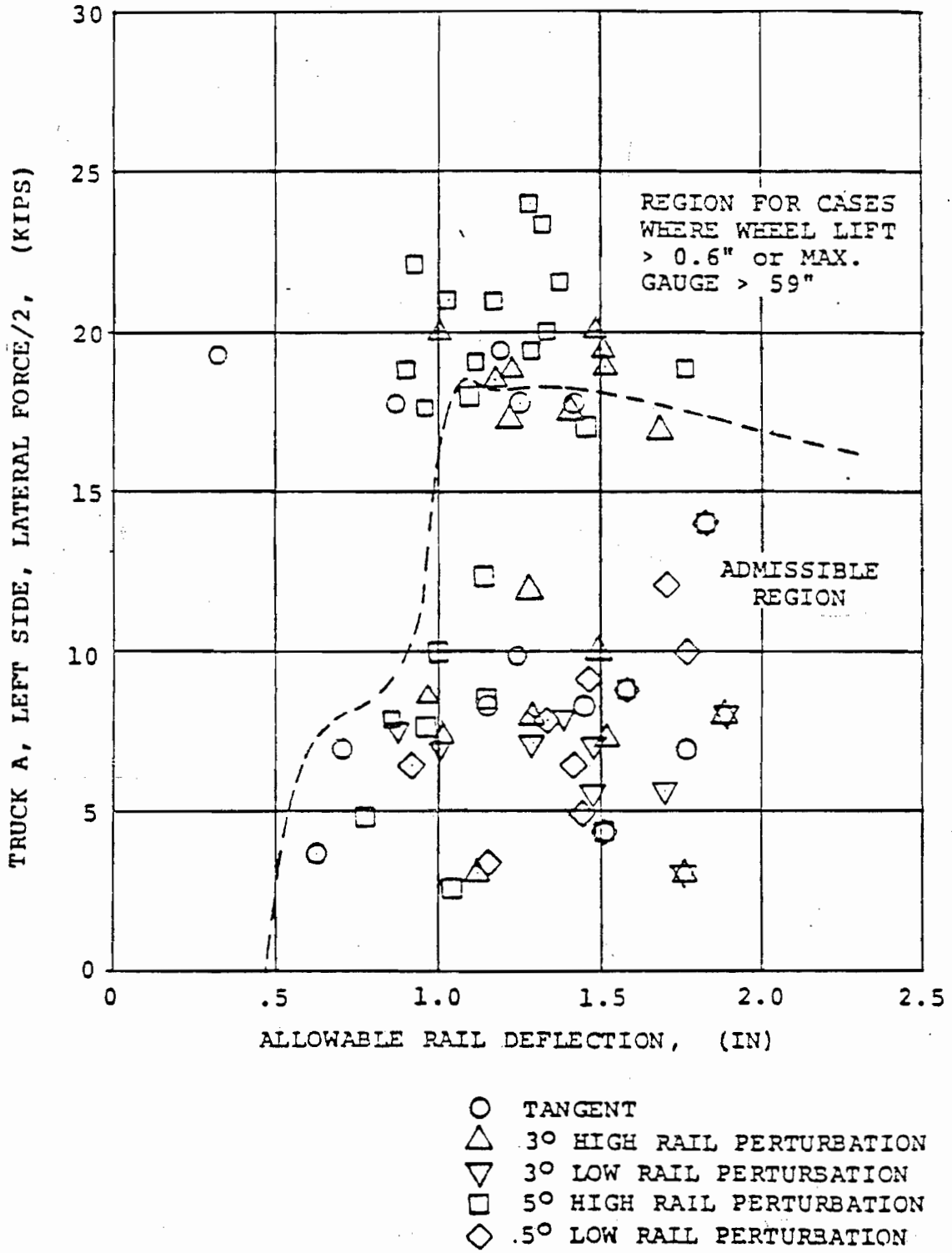

FIG. 6.3 - EXAMPLE OF RAIL RESTRAINT CAPACITY

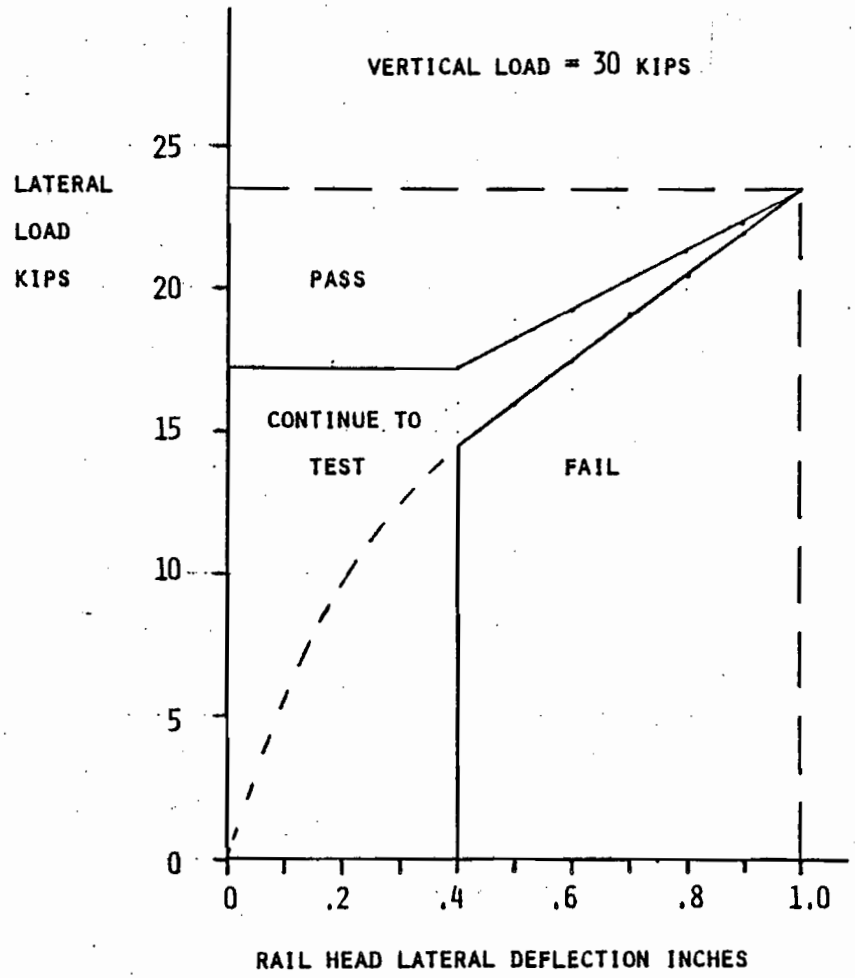

REQUIRED RAIL RESTRAINT CAPACITY

FOR TRAIN OPERATIONS AT

SPEEDS UP TO 25 MILES PER HOUR

	(A) REQUIRED LOAD	(B) TEST LOAD LIMIT
RAILHEAD DISPL.	FAIL IF L TEST IS LESS THAN:	PASS: TEST MAY BE SUSPENDED IF L TEST EXCEEDS:
LESS THAN 0.4 inches	N/A	17,250 lbs.
0.4 inches	14,500 lbs.	17,250 lbs.
0.5	16,000	18,300
0.6	17,500	19,350
0.7	19,200	20,400
0.8	20,500	21,400
0.9	22,000	22,450
1.0	23,500	23,500

FIG. 6.4 – PROTOTYPE RAIL RESTRAINT SPECIFICATION

From the analytical model different track conditions were simulated in terms of lateral rail restraint. These responses are compared to the proposed specification curve and the observations are summarized as follows:

- mimimum capacity (i.e., lower bound) track fails capacity for one missing tie
- single tie insertion or gauge bar rectifies minimum track
- upper bound track fails required capacity for three missing ties
- reinforcing lateral tie stiffness is the most effective remedy.

Recall, however, that the analytical procedures are based on the experimentally measured capacity of limiting tie conditions as found in the Logan field test. Consequently, the load levels in the qualifying test are characteristic of the response of track conditions considered minimally adaquate for service at 5-25 mph. Figure 6.5 summarizes the load-deflection response of several weak track conditions. As can be seen only severely weakened track fails to meet the load capacity reqirements included in the specification.

On going research is continuing in the area of lateral rail restraint. The additional requirements needed to fully explore gauge widening are:

1. Extension of the specification to higher speed track
2. Trial application of low speed specification
3. Prototype compliance method
4. Inclusion of provision for train handling loads
5. Low speed vehicle-track interaction load verification.

The last of these items addresses the deficiency in the available data due to the following:

- little data on cars most frequently involved in rail restraint derailments (high center of gravity)
- no data on truck loads for car types of interest
- no data in the speed range and track conditions and geometry of interest

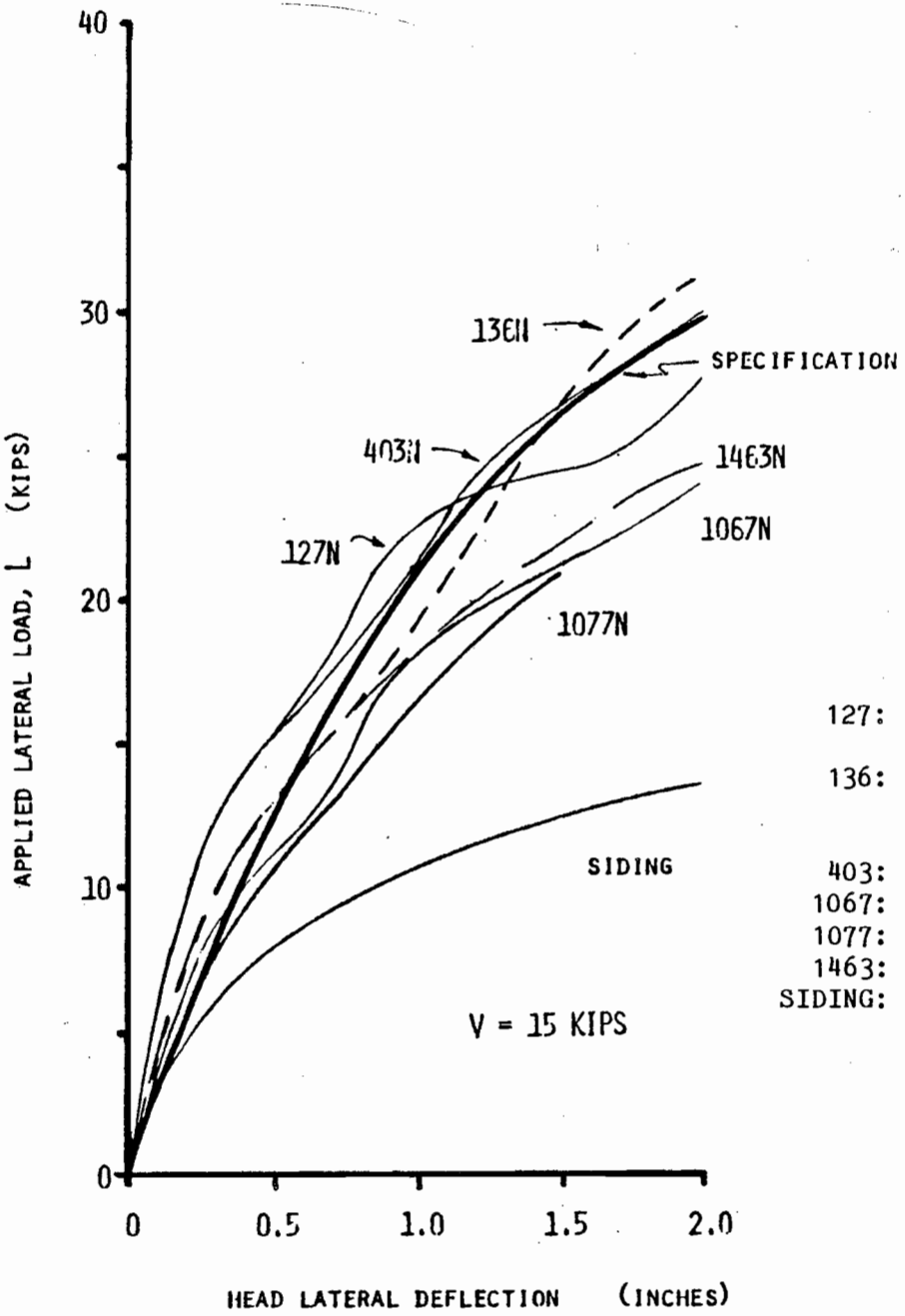

TIE DESCRIPTION

127:	DEGRADED TIE; ADJACENT TIE DEGRADED; TIE #126 MOVED AGAINGT TIE #125
136:	WORN NONDEFECTIVE TIE; ADJACENT TIES NONDEFECTIVE; AFTER 1st CYCLE WITH V=5 KIPS
403:	DEGRADED TIE; ADJACENT TIES DEGRADED
1067:	TIE #1066, #1067, AND #1068 REMOVED
1077:	TIE #1077 AND #1078 REMOVED
1463:	GOOD TIE; JOINT BOLTS REMOVED
SIDING:	(90 lb. rail) TIE DESTROYED; ADJACENT TIES DEGRADED

FIG. 6.5 - COMPARISON OF LOWER BOUND TEST RESULTS TO SPECIFICATION CURVE

- no pointwise correlation of geometry car type and loads (except Perturbed Track Test)

As a result, continuing work in this area must rely on the validated analyses which must eventually be confirmed via vehicle-track interaction tests.

REFERENCES

1. J.R. Lundgren, Lateral Strength of Track: Static Gauge Widening Tests, October 1972, Canadian National Railways Report, December 1972.

2. J. Choros, A.M. Zarembski, and I. Gitlín, Laboratory Investigation of Track Gauge Widening Characteristics, AAR Technical Center Report, September 1979.

3. J. Choros, Cyclic Gauge Widening Test Results, AAR Technical Center, 1980

4. F.B. Blader, Analytical Studies of the Relationship Between Track Geometry Variations and Derailment Potential at Low Speed, DTRS-57-80-C-00062, (Final report to be published).

5. A.M. Zarembski, Rail Rollover, The State of the Art, AAR Report No. R-288, February 1977.

6. S. Timoshenko, Method of Analysis of Statical and Dynamical Stresses in Rail, Proceedings of the 2nd International Congress for Applied Mechanics, Zurich, September 1926.

7. M.H. Bhatti, Dynamic Analysis of Rail Overturning, M.S. Thesis (Civil Engineering), Illinois Institute of Technology, December 1978.

8. K.H. Chu and Y.S. Wang, Investigation of Rail Overturning, Structural Series Report 77-2002, Department of Civil Engineering, Illinois Institute of Technology, May 1978.

9. K.H. Chu and Y.S. Wang, Investigation of Rail Overturning, Interim report, Illinois Institute of Technology, September 1976.

10. S. Timoshenko and B.F. Langer, Stresses in Railroad Track, ASME Transactions, Vol.54, 1932, pp. 277-293.

11. D.P. McConnell and A.B. Perlman, An Investigation of the Structural Limitations of Railroad Track, Draft Interim Report, Tufts University, July 1979.

12. A.B. Perlman, B.R. Lewin, and L.R. Toney, Rail Section Properties, Draft FRA Interim Report, June 1980.

13. F. Bleich, Buckling Strength of Metal Structures, McGraw-Hill, New York, 1952.

14. P. Tong and J.N. Rossettos, Finite Element Method, Basic Technique and Implementation, M.I.T. Press, 1977.

15. W. So, J.A. Hadden, H.D. Harrison, M.D. Kurre, Field Tests of Rail Restraint Capacity, Technical Memorandum, Battelle Columbus Laboratories, August 1980.

16. J.A. Hadden and M.D. Kurre, Laboratory Evaluation of Rail Restraint Characteristics, Technical Memorandum, Battelle Columbus Laboratories, July 1980.

17. A. Kish, D. Dzwonczyk, and D.Y. Jeong, Experimental Investigation of Gauge Widening and Rail Restraint Characteristics, Transportation Systems Center, Cambridge MA, 1983 (to be published)

114 copies